DOI:
10.2337/db19-0157

Document Version
Peer reviewed version

American Diabetes Association. diabetes

Overexpression of circulating soluble Nogo-B improves diabetic kidney disease by protecting the vasculature

Journal:	*Diabetes*
Manuscript ID	DB19-0157.R2
Manuscript Type:	Original Article: Complications
Date Submitted by the Author:	03-Jun-2019
Complete List of Authors:	Hernandez, Ivan; King's College London, School of Cardiovascular Medicine & Sciences Pan, Jiaqi; King's College London, School of Cardiovascular Medicine & Sciences Ricciardi, Carlo Alberto; King's College London, School of Cardiovascular Medicine & Sciences Bai, Xiaoyan; Southern Medical University Nanfang Hospital, National Clinical Research Center for Kidney Disease Ke, Jianting; King's College London, School of Cardiovascular Medicine & Sciences White, Kathryn; University of Newcastle upon Tyne, Electron Microscopy Unit Flaquer, Maria; King's College London, School of Cardiovascular Medicine & Sciences Fouli, Georgia; King's College London, School of Cardiovascular Medicine & Sciences Argunhan, Fulye; King's College London, School of Cardiovascular Medicine & Sciences Hayward, Anthea; King's College London, School of Cardiovascular Medicine & Sciences Hou, Fan Fan; Southern Medical University Nanfang Hospital, National Clinical Research Center for Kidney Disease Mann, Giovanni; King's College London, School of Cardiovascular Medicine & Sciences Miao, Robert; Medical College of Wisconsin Long, David; University College London, Developmental Biology and Cancer Programme gnudi, luigi; King's College London, School of Cardiovascular Medicine & Sciences

Overexpression of circulating soluble Nogo-B improves diabetic kidney disease by protecting the vasculature

Ivan Hernandez-Diaz[1], Jiaqi Pan[1*], Carlo Alberto Ricciardi[1*], Xiaoyan Bai[2], Jianting Ke[1~], Kathryn E White[3], Maria Flaquer[1], Georgia E Fouli[1], Fulye Argunhan[1], Anthea E Hayward[1], Fan Fan Hou[2], Giovanni E Mann[1], Robert Q Miao[4], David A Long[5], Luigi Gnudi[1^].

[1]School of Cardiovascular Medicine & Sciences, King's British Heart Foundation Centre of Research Excellence, King's College London, SE1 9NH, UK; [2]Clinical Research Centre for Kidney Disease, State Key Laboratory of Organ Failure Research, Nanfang Hospital, Southern Medical University, Guangzhou, 510515, PR China; [3]Electron Microscopy Unit, University of Newcastle upon Tyne, NE2 4HH, UK; [4]Medical College of Wisconsin, Milwaukee, WI 53226, USA; [5]Developmental Biology and Cancer Programme, Great Ormond Street Institute of Child Health, University College London, WC1N 1EH, UK.

*contributed equally

~Current address: Department of Nephrology, the Fifth Affiliated Hospital of Sun Yat-Sen University, Guangdong, China.

^Corresponding Author:
Luigi Gnudi, MD, PhD, FRCP, FASN
School of Cardiovascular Medicine & Sciences, British Heart Foundation Centre of Research Excellence, Faculty of Life Sciences & Medicine, King's College London,
150 Stamford Street, London, SE1 9NH, UK.
Phone + 44 20 78484413
Fax + 44 20 78484567
E-mail : luigi.gnudi@kcl.ac.uk

Word count
Main text: 4269
Figures: 7; Tables: 1
Supplement Material: Figures: 4; Tables: 2

Abstract

Damage to the vasculature is the primary mechanism driving chronic diabetic microvascular complications such as diabetic nephropathy which manifests as albuminuria. Therefore, treatments that protect the diabetic vasculature have significant therapeutic potential. Soluble Neurite outgrowth inhibitor-B (sNogo-B) is a circulating N-terminus isoform of full-length Nogo-B which plays a key role in vascular remodelling following injury. However, there is currently no information on the role of sNogo-B in the context of diabetic nephropathy. We demonstrate that overexpression of sNogo-B in the circulation ameliorates diabetic kidney disease by reducing albuminuria, hyperfiltration, abnormal angiogenesis and protecting glomerular capillary structure. Systemic sNogo-B overexpression in diabetic mice also associates with dampening VEGF-A signalling and reducing eNOS, AKT and GSK3β phosphorylation. Furthermore, sNogo-B prevented the impairment of tube formation which occurred when human endothelial cells were exposed to sera from patients with diabetic kidney disease. Collectively, these studies provide the first evidence that sNogo-B protects the vasculature in diabetes and may represent a novel therapeutic target for diabetic vascular complications.

Diabetic nephropathy (DN), the leading cause of end-stage renal disease in the Western world, is characterised by structural changes in the kidney glomerular filtration barrier (1; 2). This leads to enhanced glomerular permeability manifested as albuminuria, representing a common mechanism for renal and extrarenal diabetic vascular complications (3).

A complex network of vascular growth factors regulates the permeability and structure of the glomerular capillary filtration barrier (4). Glomerular levels of vascular endothelial growth factor-A (VEGF-A) and angiopoietin-2 (Angpt2) are upregulated in the early stages of DN whilst angiopoietin-1 (Angpt1) is downregulated (5-7); a milieu associated with vascular remodelling, endothelial proliferation and increased capillary permeability (1; 4). Blockade of VEGF-A signalling (8) or restoration of Angpt1 levels in podocytes (7) ameliorates albuminuria and glomerular damage in rodent models of early DN. The effects of vascular growth factors on endothelial permeability in DN are partly mediated by nitric oxide (NO) signalling through modulation of endothelial nitric oxide phosphorylation ($eNOS^{Ser1177}$) which acts in an AKT-dependent manner (9). In diabetes, reduction in NO availability due to eNOS uncoupling (10) has been implicated in the pathophysiology of DN. Podocyte-specific overexpression of *Angpt1* activates eNOS (7) in diabetic mice, whilst the beneficial effect of VEGF-A blockade on albuminuria in DN is prevented in *eNOS* knock-out mice (11).

Another pathway involved in vascular remodelling is the neurite outgrowth inhibitor (Nogo) family which is encoded by one gene with three major isoforms: Nogo-A, -B and -C (12), mainly expressed in the endoplasmic reticulum (ER)(13). Nogo-A and -C are found in the central nervous system and muscle tissue respectively, whilst Nogo-B localises to endothelial and smooth muscle cells within the vasculature (12). In physiology, loss of Nogo-B upregulates eNOS-NO and flow-mediated vasodilation, leading to hypotension (14). Mice lacking both Nogo-A and B are viable and do not have major apparent vascular defects (15). However, vascular lesions are enhanced in Nogo A/B deficient mice following injury which can be prevented by gene delivery of full-length Nogo-B (15; 16).

The full-length Nogo-B protein of 49 kDa can be cleaved into a shorter ~150-aa N-terminus fragment (17) which can then be secreted into the circulation as soluble Nogo-B (sNogo-B)(18). This Nogo-B N-terminus (identical in circulating sNogo-B and full-length Nogo-B within

the cells) binds to its receptor NgBR, expressed in endothelial cells on the cell plasma membrane and in the ER leading to endothelial cell proliferation/vascular remodelling (15; 19), angiogenesis during development, vascular repair, and cytoskeletal organisation (12; 20-23). Given the role of this N-terminal fragment of Nogo-B in vascular remodelling, we hypothesised that overexpression of sNogo-B in the circulation could have a protective role in the setting of diabetic kidney disease.

Research design and methods

Materials and chemicals were purchased from Sigma (Gillingham, UK) and Starlab (Milton Keynes, UK) unless otherwise stated.

Experimental animal model of diabetes

To induce diabetes, 8-10 week old (~20g in weight) male DBA2J mice were administered with streptozotocin (low dose multiple injection protocol)(7; 8). Mice were considered diabetic with a fed glycemia >22 mmol/l. Control non-diabetic littermates were injected with vehicle only (citrate buffer). Two weeks later, some diabetic and non-diabetic mice were administered an Adeno Associated viral Vector expressing 6xHis-Tag/sNogo-B (AAV-sNogo-B)(**Supplemental Material, Fig. 1a)**. The utilised vector, AAV/DJ, has a specific tropism for the liver and maintains a sustained expression of transgene for 15-17 weeks under the CMV promoter (24). The construct also contains a secretory alkaline phosphatase peptide, which drives the release of the 6xHis-Tag/sNogo-B protein in the circulation. To control for infection, other diabetic and non-diabetic mice were injected with AAV/DJ driving the expression of green fluorescent protein (GFP) under the same promoter (AAV-GFP).

All mice were maintained for 12-14 weeks after induction of diabetes before sacrifice and tissues analysis. Prior to sacrifice, blood pressure was assessed with tail cuff methodology, and 24h-urine collection was conducted with mice kept in metabolic cages for creatinine, sNogo-B and albuminuria determination (7). At sacrifice full blood and plasma was collected (to assess for HbA1c, creatinine by high performance liquid chromatography, and sNogo-B levels). Kidney tissue was harvested for histology, electron microscopy (EM), and lysates of kidney cortex or isolated glomeruli frozen for further analysis (7).

Immunofluorescence

Proliferating glomerular ECs (GECs) determination

Glomerular Ki67/CD31 and CD31-positive GECs per glomerulus were visualised with fluorescent microscope (7); an average of 30-40 glomeruli per animal were studied and the means values utilised in the analysis.

Endothelial glycocalyx determination

Lectin staining was assessed as indicator of thickness/integrity of the endothelial glycocalyx in frozen kidney sections as described (25). A total of 10-15 capillary loops were analysed per mouse from 5-7 glomeruli and the mean value for each animal was utilised in the analysis.

Electron microscopy and glomerular ultrastructure analysis

Mesangial volume fraction, GBM thickening, podocyte number and glomerular volume were studied as described (7; 8). For detailed methodology see Supplemental Material.

sNogo, VEGF-A, Angpt1/2 and VEGFR2^{Tyr1173} phosphorylation ELISA

sNogo-B in plasma, urine and cell culture media was assessed by ELISA (BioLegend, San Diego, CA, USA). ELISA was also utilised for kidney cortex VEGF-A (R&D Systems, Abingdon, UK), Angpt1/2 (Biomatick, Wilmington, DE, USA) and VEGFR2 phosphorylation (PathScan, Cell Signalling, Leiden, The Netherlands) levels; results were normalised for mcg of total kidney cortex protein lysates.

Immunoblotting

Immunoblotting was performed on cells and tissues lysates (mouse renal cortex and isolated glomeruli) as described (7). The following primary antibodies were utilised: Nogo-B (N-terminus, R&D System, Abingdon, UK); NgBR (Abcam, Cambridge, UK); α-tubulin (Santa Cruz Biotechnology, Heidelberg, Germany); β-actin; pan-AKT, GSK3β, phospho-AKT (Ser^{473}), phospho-eNOS (Ser^{1177}), and phospho-GSK3β^{Ser9} (Cell Signalling, Leiden, The Netherlands); eNOS (Santa Cruz Biotechnology, Heidelberg, Germany); total β-catenin (Proteintech, Manchester, UK).

Culture of mouse lung endothelial cells, human GECs, and human podocytes

Primary lung ECs were isolated from adult C57BL/6J mice and cultured, up to three passages, as described (14).

Human GECs and podocytes were cultured as described (26; 27). To examine the effect of high glucose and VEGF-A in fully differentiated GECs, cells were starved for 12h in 1% serum followed by incubation in normal glucose (5 mmol/l glucose+20 mmol/l mannitol) or high glucose (25 mmol/l glucose) for 72h in the presence or absence of VEGF-A (50 ng/ml).

Immunoprecipitation (IP) and proximity ligation assay (PLA) experiments

For IP experiments, GEC were transfected with 6xHis-Tag/sNogo-B adenovirus (ADV-sNogo-B - transgene identical to the AAV-sNogo-B construct) at 100 multiplicity of infection (MOI) for 4h and studied after 24h; whole protein lysates were obtained and incubated with either anti NgBR (Novus Biological, Oxford, UK), or anti 6xHis-Tag antisera (ThermoFisher Scientific, Oxford, UK), or vehicle IgG. Immunoblotting was conducted on immunoprecipitates obtained with anti-6xHis-Tag and -NgBR antisera.

For the PLA experiments cell culture media enriched with 6xHis-Tag/sNogo-B was obtained by transfecting confluent human GECs with ADV-sNogo-B (100 MOI) in full media for 4h; subsequently cells were put in 1% serum media and supernatant (containing 6xHis-Tag/sNogo-B protein, ~6000 pg/ml) collected after 48h; collected media was stored at 4°C and utilised within 6-12h. Human differentiated GECs were then incubated with "6xHis-Tag/sNogo-B conditioned media" for 1, 5 and 15min, fixed in 4% paraformaldehyde for 10min, and then incubated with primary antisera against NgBR (1:100 dilution, rabbit anti N-terminus NgBR, gift from R. Miao), and anti 6xHis-Tag (1:100 dilution) mouse monoclonal antiserum (ThermoFisher Scientific, Oxford, UK). The NgBR-sNogo-B interaction was visualised with immunofluorescence following manufacturer instructions (Duolink® In Situ Red Starter Kit Mouse/Rabbit).

Nogo-B immunogold staining in glomeruli

Nogo-B immunogold staining was conducted in mouse renal cortex tissue as previously described using a sheep polyclonal anti-Nogo-B (N-terminus) antibody (R&D System, Abingdon, UK)(8).

Nogo-B immunohistochemistry

Nogo-B immunohistochemistry was conducted in mouse and human (patients with DN or thin basement membrane nephropathy-TBMN)(**Supplemental Material, Table 1**) kidney tissue paraffin sections using the streptavidin-biotin complex method with specific sheep polyclonal anti Nogo-B N-terminus antibody (R&D System, Abingdon, UK).

In human tissue, Nogo-B expression was quantified by assessing the % glomerular area with positive staining. Ten glomeruli were analysed for each human biopsy and the calculated average Nogo-B staining/area of glomeruli was then used for analysis.

Role of sNogo-B overexpression in human umbilical vein endothelial cells (HUVEC) tube formation assay

To examine the continuous paracrine/autocrine effect of sNogo-B on angiogenesis, HUVEC were transfected with ADV-sNogo-B or identical vector lacking sNogo-B cDNA (control vector)(**Supplemental Material, Fig. 1b**) for 4h; cells were then equilibrated (24h) in complete medium and then plated in 96 well plates (5000 cells/well) in EGM basal media containing sera (4% vol/vol) obtained from patients with type-1 diabetes (T1DM) susceptible (DN+) or protected (DN-) towards the progression of DN (**Supplemental Material, Table 2**). Tube formation was performed on Matrigel (BD Biosciences, UK)(28) in duplicate and assessed after 24h. Tube length and number were analysed in a blinded fashion with the Wimasis WimTube image system (29).

Statistical Methods

Differences among groups were analysed by two tails Student's t-test or ANOVA with post-hoc Least Significant Difference (LSD) pairwise comparisons test for normally distributed variables. Kruskal-Wallis and Mann-Whitney non-parametric tests were used for not normally distributed variables (albuminuria and sNogo-B). Data are expressed as means±standard deviation (SD) for normally distributed data or as median and interquartile range for not

normally distributed data. Analysis was conducted with IBM SPSS-22 software (New York, NY, USA) and statistical significance was accepted at $p \leq 0.05$.

Results

sNogo-B overexpression ameliorates diabetes-mediated albuminuria and hyperfiltration

Non-diabetic (ND) and diabetic (D) mice injected with AAV-sNogo-B were characterised by a 12-fold increase in circulating sNogo-B when compared with those injected with control vector (AAV-GFP)(**Fig. 1a**, ND-GFP *vs* ND-sNogo-B, p=0.00001; D-GFP *vs* D-sNogo-B, p=0.0001). Diabetes led to a significant increase in HbA1c levels (ND-GFP *vs* D-GFP, p=0.00008; ND-sNogo-B *vs* D-sNogo-B, p=0.00004), which was paralleled by a loss of body weight (ND-GFP *vs* D-GFP, p=0.0001; ND-sNogo-B *vs* D-sNogo-B, p=0.00001), increased kidney/body weight ratio (ND-GFP *vs* D-GFP, p=0.006; ND-sNogo-B *vs* D-sNogo-B, p=0.0002) and a modest decrease in systolic blood pressure (ND-GFP *vs* D-GFP, p=0.01; ND-sNogo-B *vs* D-sNogo-B, p=0.003)(**Table 1**).

Glomerular permeability, measured by albumin excretion rate over 24h urine collection, was increased in diabetic mice compared with non-diabetic mice (**Fig. 1b**, ND-GFP *vs* D-GFP, p=0.0001). Overexpression of sNogo-B in the circulation of diabetic mice led to a significant 40-50% reduction in albuminuria (**Fig. 1b**, D-GFP *vs* D-sNogo-B, p=0.04). This effect was independent of changes in systemic blood pressure, kidney/body weight and glycaemic control which were similar in diabetic mice administered either AAV-sNogo-B or AAV-GFP (**Table1**). Diabetes-mediated renal hyperfiltration was evidenced by raised creatinine clearance levels (**Fig. 1c**, ND-GFP *vs* D-GFP, p=0.02) and AAV-sNogo-B overexpression attenuated this effect (**Fig. 1c**, D-GFP *vs* D-sNogo-B, p=0.04).

Urinary sNogo-B was measured in a subset of animals. Diabetes was paralleled by an increase in 24h-urine sNogo-B in both mice administered AAV-GFP or AAV-sNogoB (**Fig. 1d**, ND-GFP *vs* D GFP and ND-sNogo-B *vs* D-sNogo-B, p≤0.002); no differences were observed in urine sNogo-B between AAV-GFP or AAV-sNogo-B mice within the ND and D group.

Effects of sNogo-B overexpression on GECs and podocytes in diabetes

The results above implicate sNogo-B as having a protective role in glomerular capillary permeability in diabetic kidneys. We therefore explored whether elevated circulating levels of

sNogo-B might stabilise the glomerular vasculature and confer a healthier GEC and podocyte phenotype in diabetes.

Firstly, we examined GECs proliferation to assess the effect of sNogo-B on abnormal vascular remodelling that occurs in early diabetic glomerulopathy (**Fig. 2a, b**)(1; 7). Diabetes increased the number of $CD31^+/Ki67^+$ cells per glomerulus by 7-fold which was attenuated in mice with sNogo-B overexpression in the circulation (**Fig. 2b**, ND-GFP *vs* D-GFP, p=0.0001; D-GFP *vs* D-sNogo-B, p=0.005). The total number of $CD31^+$ cells/glomeruli was not different between animals with increased sNogo-B in the circulation in either non-diabetic and diabetic mice (mean±SD CD31+ cells/glomeruli: ND-GFP 7.6±1.37, ND-sNogo-B 7.7±1.8, D-GFP 9.7±2.4, D-sNogo-B 9.5±3.0, n=7 animals per group, p=ns).

We performed lectin staining as an indicator of thickness/integrity of the glomerular endothelial glycocalyx, which is known to contribute to vascular permeability (30). The estimated lectin thickness was significantly reduced in diabetic mice but restored to base-line levels in mice administered AAV-sNogo-B (**Fig. 2c**, ND-GFP *vs* D-GFP p=0.009; D-GFP *vs* D-sNogo-B, p=0.0004).

Using EM (**Supplementary Material, Fig. 2**), we found that diabetes was also paralleled by a significant decrease in the number of podocytes per glomerulus (**Fig. 2d**, ND-GFP *vs* D-GFP p=0.0002), increased the mesangial volume fraction (**Fig. 2e**, ND-GFP *vs* D-GFP p=0.02) but had no effect on glomerular basement membrane (GBM) width (**Fig. 2f**) or glomerular volume (**Table 1**). The reduction in podocyte number observed in diabetic mice was ameliorated by elevated circulating sNogo-B levels (**Fig. 2d**, D-GFP *vs* D-sNogo-B, p=0.01). Overexpression of sNogo-B in the circulation did not alter diabetes-mesangial expansion (**Fig. 2e**), GBM width (**Fig. 2f**), or glomerular volume in diabetic mice (**Table 1**).

Effects of sNogo-B overexpression in the circulation on vascular growth factors, eNOS, AKT and GSK3β signalling in the kidney cortex

To identify the molecular mechanisms by which sNogo-B might alter the endothelium in diabetes, we examined levels of the vascular growth factors VEGF-A, Angpt1 and Angpt2 in kidney cortex lysates. VEGF-A protein levels were significantly increased in diabetic mice (**Fig.**

3a, ND-GFP *vs* D-GFP, p=0.009) and were reduced when sNogo-B was overexpressed in the circulation (**Fig. 3a**, D-GFP *vs* D-sNogo-B, p=0.03).

In accord with these findings, phosphorylation levels of the main VEGF-A receptor, VEGFR2, in the kidney cortex were significantly elevated in diabetic mice; an effect which was dampened in mice with elevated circulating sNogo-B levels (**Fig. 3b**, ND-GFP *vs* D-GFP, p=0.003; D-GFP *vs* D-sNogo-B, p=0.01). Angpt1/Angpt2 ratio was lower in diabetic mice and was not altered by sNogo-B overexpression in the circulation (**Fig. 3c**, ND-GFP *vs* D-GFP, p=0.03; ND-sNogo-B *vs* D-sNogo-B, p=0.001).

Given that upregulation of sNogo-B in the circulation was paralleled by altered VEGF-A signalling, whose effects on endothelial permeability in DN are regulated by eNOS activation (9), we examined phosphorylation of eNOS. Diabetes led to a significant increase in the ratio of phosphorylated eNOSs^{Ser1177}/total eNOS (**Fig. 3d-e**, ND-GFP *vs* D-GFP, p=0.017) which was prevented by sNogo-B overexpression (**Fig. 3d-e**, D-GFP *vs* D-sNogo-B, p=0.05). As protein kinase B (AKT) activation is involved in endothelial cell proliferation and eNOS phosphorylation (9) we investigated the phosphorylation at the AKT^{Ser473} site. The ratio of AKT^{Ser473} phosphorylation/total AKT was upregulated in diabetic mice; an effect which was significantly attenuated in mice injected with AAV-sNogo-B (**Fig. 4a**, ND-GFP *vs* D-GFP, p=0.0001; D-GFP *vs* D-sNogo-B, p=0.04). The level of total AKT protein was downregulated by diabetes (ND-GFP *vs* D-GFP, p=0.002)(31), but elevated circulating levels of sNogo-B had no effect on total AKT protein expression in kidney cortex lysate.

We then investigated activation of GSK3β, a known substrate of AKT (32), that has been postulated as a therapeutic target for diabetic glomerulopathy (33). The ratio of phosphorylated GSK3β^{Ser9}/total GSK3β was upregulated in kidney cortex lysates of diabetic mice when compared with non-diabetic mice (**Fig. 4b**, ND-GFP *vs* D-GFP, p=0.006) consistent with previous reports (33). Notably, sNogo-B overexpression in the circulation was paralleled by a significant downregulation of GSK3β^{Ser9} phosphorylation/total GSK3β in diabetic mice (**Fig. 4b**, D-GFP *vs* D-sNogo-B, p=0.04). Total GSK3β protein expression was not altered in any of the experimental groups studied. As a known substrate of GSK3β, and important player in DN (34), we studied total β-catenin (35) protein levels in kidney cortex

lysate. In line with GSK3β activation status, β-catenin was significantly upregulated in diabetic mice when compared to non-diabetic mice (**Fig. 4c**, ND-GFP *vs* D-GFP, p=0.007). sNogo-B overexpression in the circulation led to a significant downregulation of β-catenin in kidney cortex of diabetic mice, (**Fig. 4c**, D-GFP *vs* D-sNogo-B, p=0.01), whereas β-catenin protein levels were unaffected in non-diabetic animals.

sNogo-B binds to NgBR in human GECs in vitro.

Next, we examined the physical interaction between sNogo-B and NgBR by IP and PLA experiments in human GECs (26). Firstly, we showed that GECs expressed NgBR *in vitro*. We then could detect an interaction between 6xHis-Tag/sNogo-B and NgBR with IP experiments (**Supplemental Material, Fig. 3a**).

The sNogo-B/NgBR interaction was further confirmed with PLA experiments where the sNogo-B/NgBR interaction was observed by identification of positive red/orange dots signals in GECs incubated with “conditioned media” containing sNogo-B protein as early as 1min (**Supplemental Material, Fig. 3b**).

Renal cortical levels of full-length Nogo-B are downregulated in an animal model of diabetes and restored by sNogo-B overexpression in the circulation

To further explore the reno-protective mechanisms of sNogo-B overexpression in the circulation we investigated the expression of full-length Nogo-B in mouse and human kidney tissue in diabetes. With immunogold staining, combined with electron microscopy, we found that full-length Nogo-B protein was localised in both GECs and podocytes in non-diabetic male adult mice (**Fig. 5a**). Immunohistochemical staining confirmed the expression of full-length Nogo-B in the glomerular tuft and, as described, in cortical collecting duct (**Fig. 5b**)(36). Full-length Nogo-B protein, assessed by immunoblotting, in glomeruli enriched kidney cortex and isolated glomeruli lysates was 2-3-fold downregulated in diabetic mice when compared with non-diabetic controls (**Fig. 5c**, ND-GFP *vs* D-GFP, p≤0.045); sNogo-B overexpression in the circulation restored the diabetes-induced loss of full length Nogo-B (**Fig. 5c**, D-GFP *vs* D-

sNogo-B, p≤0.015). NgBR was expressed in isolated glomeruli but not modulated by diabetes or elevated sNogo-B circulating levels (**Fig. 5d**).

We also investigated the expression of full-length Nogo-B in human kidney biopsies obtained from two distinct glomerular diseases: DN and TBMN. DN represents a progressive proteinuric disease, while TBMN represents a benign non-proteinuric, non-progressive disorder, featuring a uniformly thinned GBM (37) without any other significant glomerular pathology (**Supplemental Material, Table 1**). Nogo-B expression was lower in glomeruli of kidney biopsies of patients with DN when compared with patients with TBMN (**Fig. 5e,** TBMN *vs* DN, p=0.0001).

High glucose and VEGF-A promote full-length Nogo-B downregulation and increased sNogo-B secretion in the supernatant of GECs in culture

Fully differentiated human GECs (26) incubated in normal (NG) or high glucose (HG) condition, with VEGF-A (50 ng/ml, or vehicle) or a combination of HG and VEGF-A for 72h, showed a 30-40% downregulation of full-length Nogo-B expression (NG *vs* HG, NG *vs* VEGF-A, NG *vs* HG+VEGF-A, p≤0.04)(**Fig. 6a**). HG and/or VEGF-A-mediated full length Nogo-B downregulation was paralleled by an upregulation of sNogo-B secretion in the supernatant (NG *vs* HG, NG *vs* VEGF-A, NG *vs* HG+VEGF-A, p≤0.03)(**Fig. 6b**).

sNogo-B overexpression corrects altered tube formation seen in HUVEC cultured with T1DM/DN+ serum

Finally, we explored the paracrine/autocrine effects of secreted sNogo-B overexpression on the ability of HUVEC, known to express NgBR (19), to differentiate in a tube-like structure (tube formation assay)(38) when incubated with the serum of patients with T1DM with (DN+) or without (DN-) DN (**Supplemental Material, Table 2**).

sNogo-B overexpression led to a 5-fold increase in sNogo-B released from cells into the supernatant when compared with ADV-control transfected cells (**Fig. 7d,** ADV-control *vs* ADV-sNogo-B within DN- and DN+, p=0.0001).

HUVECs incubated with serum of patients with T1DM/DN+ had decreased numbers and lengths of tubes when compared to cells incubated with serum of patients with T1DM/DN- (**Fig. 7a**, **b, c,** ADV-control, DN^- *vs* DN^+, tube length p=0.01, tube number p=0.04). Increased sNogo-B in the supernatant was paralleled by a correction of the impaired tube formation observed in cells incubated with DN+ serum (**Fig. 7a, b, c,** DN+, ADV-control *vs* ADV-sNogo-B, tube length p=0.02, tube number p=0.001).

Discussion

In this study, we demonstrated, in DBA2/J diabetic mice, that systemic overexpression of the N-terminal fragment sNogo-B, which binds to NgBR, improved diabetic glomerulopathy as evidenced by a reduction in albuminuria. This finding was associated with reduced GECs proliferation, restoration of glycocalyx thickness, maintenance of podocyte number and dampening of VEGF-A signalling and eNOS, AKT and GSK3β phosphorylation as assessed in glomeruli enriched kidney cortex lysates. Finally, sNogo-B prevented the impairment of tube formation which occurred when endothelial cells were exposed to sera from T1DM patients with DN.

The reduction in diabetes-mediated albuminuria seen in mice with sNogo-B overexpression in the circulation was possibly partly driven by a parallel fall in diabetes-mediated glomerular hyperfiltration; this was not accompanied by an increase in glomerular volume, which is in accord with other reports examining the early (up to 16 weeks of diabetes) phase of DN in DBA2J mice (39). Other potential confounders for the reduced albuminuria could be that sNogo-B overexpression in the circulation lowers blood pressure or be related to changes in glycaemic control (2). However, we did not find any change in systemic blood pressure or glycaemic control between diabetic mice with overexpression of sNogo-B in the circulation or control mice ruling out these possibilities. As previously described the blood pressure observed in diabetic DBA2J mice was slightly lower than in non-diabetic ones (39).

Urinary sNogo-B was elevated in diabetes, likely due to the increased permeability of the filtration barrier. However, the excretion of sNogo-B was not increased in either non-diabetic or diabetic mice administered AAV-sNogoB; a finding most likely to be attributed to the large molecular weight of the 6xHis-Tag/sNogo-B (~80 kDa, **Supplemental Material, Fig. 1c)**.

As albuminuria results from defects in the glomerular filtration barrier, we initially focussed on the glomerular endothelium since the biological effects of sNogo-B and its receptor NgBR are primarily on the vasculature (14; 19). Elevated circulating levels of sNogo-B prevented diabetes-mediated glomerular endothelial cell proliferation as seen in the early stages of DN (1; 7; 40). sNogo-B overexpression in the circulation was also associated with amelioration of the diabetes-induced loss of lectin, an important component of the endothelial glycocalyx,

known to contribute to vascular permeability (25; 41). These changes were paralleled by a reduction in VEGF-A signalling. VEGF-A is a potent stimulator of endothelial cell proliferation (42) and dampening VEGF-A signalling ameliorates albuminuria and glomerular damage in DN (4). VEGF-A has also been implicated in the regulation of the thickness of the endothelial glycocalyx in diabetic mice with the anti-angiogenic VEGF-A_{165b} isoform able to restore the diabetes-induced loss of the endothelial glycocalyx and albuminuria (41). There have been a few reports linking the sNogo-B/NgBR and VEGF-A/VEGFR2 systems suggesting a concerted vasculoprotective role (20; 43).

The effects on the endothelium may also be related to the changes seen in Wnt/β-catenin signalling. Activation of Wnt/β-catenin signaling (with cellular β-catenin accumulation) results in endothelial dysfunction, inflammation and fibrosis, and has been implicated in DN (34). Inactive GSK3β is also known to promote endothelial cell proliferation (44), with a phosphorylated (inactive) GSK3β favouring accumulation of cellular β-catenin (45), a promoter of angiogenesis and enhancer of VEGF-A/VEGFR2 signaling (46). In our experiments, we showed that sNogo-B reduced GSK3β phosphorylation/β-catenin which may contribute to preventing the angiogenesis response to diabetes-mediated vascular damage and dampen VEGF-A/VEGFR-2 signalling.

Increased eNOS phosphorylation and NO production have been implicated in hyperfiltration in the early phases of diabetic glomerulopathy (47; 48), and the role of eNOS in oxidative stress (when in an “uncoupled state”(49)) is implicated in DN and GECs/podocyte damage (50). The reduction in diabetes-mediated eNOS phosphorylation, observed in kidney cortex lysates of diabetic mice with elevated sNogo-B circulating levels, would result in reduced eNOS-mediated NO production and oxidative stress; events that could contribute to a reduction in glomerular hyperfiltration (51) and in the prevention of diabetes-mediated loss of GECs glycocalyx and podocyte detachment. sNogo-B overexpression in the circulation associates with inhibition of diabetes-mediated modulation of VEGF-A/VEGFR2 and AKT/GSK3β/β-catenin system, signalling pathways which are implicated in podocyte injury/detachment and albuminuria (52-54). Finally, it might be possible that sNogo-B may

have a direct effect on podocytes as evidenced by our *in vitro* data showing expression of NgBR in human podocyte cells (**Supplemental Material, Fig. 4**).

Full-length Nogo-B (assessed with specific N-Terminus antiserum) was found to be expressed in isolated glomeruli and glomeruli enriched kidney cortex lysates and downregulated in diabetic mice. Full-length Nogo-B expression levels were also lower in glomeruli of proteinuric DN (a progressive chronic kidney disease) biopsy kidney samples when compared with TBMN, a benign glomerular disease without proteinuria, suggesting that the presence of proteinuria/albuminuria associates with reduced glomerular full-length Nogo-B levels. Whether low glomerular Nogo-B causes albuminuria is yet to be determined, but in experimental models of diabetic retinopathy lack of full-length Nogo-B attenuated high glucose induced cell migration and tube formation (EC differentiation)(55). In contrast to our findings, studies performed in humans' and rodents' renal biopsies (NephroSeq database, University of Michigan, USA), showed no change in full-length Nogo-B mRNA expression in diabetic kidney tissue when compared with control tissue.

We also demonstrate that high glucose and/or VEGF-A determine, in GECs in culture, an increase in sNogo-B in the supernatant and a parallel reduction in cellular full length Nogo-B (probed with specific N-Terminus antiserum). These results support the cleavage of the full-length Nogo-B N-Terminus as previously described (17) and future work will have to address the mechanisms behind this phenomenon.

We then explored the putative vasculo-protective role of sNogo-B in an angiogenesis experimental model in HUVEC cultured with sera of patients with T1DM susceptible (DN+) or protected (DN-) towards the progression of DN (56). We demonstrate that circulating factors (sera from T1DM/DN+), other than glucose, negatively affect ECs tube formation and sNogo-B overexpression in the supernatant rescued this defect favouring ECs differentiation towards a stable tube structure, an effect likely related to the patients' "DN" status rather than being driven by renal impairment given that the average of renal function of the two groups of patients studied was 80-100 ml/min per 1.73m^2. Importantly, artificial upregulation of the N-terminus of Nogo-B (sNogo-B) in the supernatant is able, via a paracrine autocrine

mechanism, to ameliorate the ability of ECs to migrate and differentiate into tubule-like structures (38), which translates in a more stable vasculature.

Collectively, our studies provide the first evidence that a primary increase of sNogo-B in the circulation protects the glomerular vasculature in diabetes. More studies will need to further dissect sNogo-B mechanism/s of action and explore its potential benefit in diabetic animals with established kidney disease. sNogo-B could represent a novel targetable pathway for the treatment of diabetic chronic vascular complications.

Acknowledgements

This work was supported by BHF Project Grant PG/16/41/32138 to LG, DAL, and GEM; Heart Research UK (PhD Studentship to JP grant RG2619/12/15) to LG and DAL; Diabetes Research Wellness Foundation (start-up grant) to LG; start-up support from Henry Lester Trust to JP; MF was supported by an ERA-EDTA non-clinical fellowship; XB and FFH were supported by grants from the National Natural Science Foundation of China (no. 81100496) and Guangdong Natural Science Foundation (no. 2016A030313581); CAR was supported by visiting fellowship from the Italian Society of Nephrology and Kidney Research UK fellowship (TF_001_20171120). We also acknowledge support from National Institute for Health and Research, Biomedical Research Centre award to Guy's and St Thomas Foundation Trust in partnership with King's College London. DAL is supported by the Medical Research Council (MR/P018629/1), Diabetes UK (13/0004763, 15/0005283), Kidney Research UK (RP36/2015), and by the NIHR BRC at Great Ormond Street Hospital for Children NHS Foundation Trust and University College London.

We acknowledge Dr W Sessa (Yale University, CT, USA) for the sNogo-B construct, Dr S Satchell (Bristol University, UK) for the human GECs and Dr M Saleem (Bristol University, UK) for the human podocytes cell lines. We are grateful to the patients who participated in this research.

Authors contribution

LG and DAL conceived the experiment, IHD, DAL and LG contributed to experimental design and data collection together with CAR, JP, XB, JK, KEW, MF, GEF, FA, AEH; FFH, GEM, and RQM; LG, GEM, DAL and IHD lead data discussion, interpretation, and manuscript writing with input from all other co-Authors. All Authors have approved the final manuscript.

Guarantor statement

Dr L Gnudi is the guarantor of this work and, as such, had full access to all the data in the study and takes responsibility for the integrity of the data and the accuracy of the data analysis.

Conflict of interests' statement

The authors have declared that no conflict of interest exists.

Prior presentations

Part of this work was previously presented in abstract form at the EASD (2017,2018), ASN (2017-2019), ERA-EDTA (2017) and EDNSG (2016-2018) annual meetings.

Data and Resource Availability

The datasets generated during and/or analyzed during the current study are available from the corresponding author upon reasonable request.

The viral vectors generated during and/or analyzed during the current study is available from the corresponding author upon reasonable request.

References:

1. Nakagawa T, Kosugi T, Haneda M, Rivard CJ, Long DA: Abnormal angiogenesis in diabetic nephropathy. Diabetes 2009;58:1471-1478

2. Gnudi L, Coward RJ, Long DA: Diabetic Nephropathy: Perspective on Novel Molecular Mechanisms. Trends Endocrinol Metab 2016;27:820-830

3. Deckert T, Feldt-Rasmussen B, Borch-Johnsen K, Jensen T, Kofoed-Enevoldsen A: Albuminuria reflects widespread vascular damage. The Steno hypothesis. Diabetologia 1989;32:219-226

4. Gnudi L, Benedetti S, Woolf AS, Long DA: Vascular growth factors play critical roles in kidney glomeruli. Clin Sci (Lond) 2015;129:1225-1236

5. Cooper ME, Vranes D, Youssef S, Stacker SA, Cox AJ, Rizkalla B, Casley, Dj, Bach LA, Kelly DJ, Gilbert RE: Increased renal expression of vascular endothelial growth factor (VEGF) and its receptor VEGFR-2 in experimental diabetes. Diabetes 1999;48:2229-2239

6. Jeansson M, Gawlik A, Anderson G, Li C, Kerjaschki D, Henkelman M, Quaggin SE: Angiopoietin-1 is essential in mouse vasculature during development and in response to injury. J Clin Invest 2011;121:2278-2289

7. Dessapt-Baradez C, Woolf AS, White KE, Pan J, Huang JL, Hayward AA, Price KL, Kolatsi-Joannou M, Locatelli M, Diennet M, Webster Z, Smillie SJ, Nair V, Kretzler M, Cohen CD, Long DA, Gnudi L: Targeted Glomerular Angiopoietin-1 Therapy for Early Diabetic Kidney Disease. J Am Soc Nephrol 2014;25(1):33-42

8. Ku CH, White KE, Dei CA, Hayward A, Webster Z, Bilous R, Marshall S, Viberti G, Gnudi L: Inducible overexpression of sFlt-1 in podocytes ameliorates glomerulopathy in diabetic mice. Diabetes 2008;57:2824-2833

9. Fulton D, Gratton JP, McCabe TJ, Fontana J, Fujio Y, Walsh K, Franke TF, Papapetropoulos A, Sessa WC: Regulation of endothelium-derived nitric oxide production by the protein kinase Akt. Nature 1999;399:597-601

10. Forstermann U, Sessa WC: Nitric oxide synthases: regulation and function. Eur Heart J 2012;33:829-837, 837a-837d

11. Yuen DA, Stead BE, Zhang Y, White KE, Kabir MG, Thai K, Advani SL, Connelly KA, Takano T, Zhu L, Cox AJ, Kelly DJ, Gibson IW, Takahashi T, Harris RC, Advani A: eNOS deficiency predisposes podocytes to injury in diabetes. J Am Soc Nephrol 2012;23:1810-1823

12. Oertle T, Schwab ME: Nogo and its paRTNers. Trends Cell Biol 2003;13:187-194

13. Voeltz GK, Prinz WA, Shibata Y, Rist JM, Rapoport TA: A class of membrane proteins shaping the tubular endoplasmic reticulum. Cell 2006;124:573-586

14. Cantalupo A, Zhang Y, Kothiya M, Galvani S, Obinata H, Bucci M, Giordano FJ, Jiang XC, Hla T, Di Lorenzo A: Nogo-B regulates endothelial sphingolipid homeostasis to control vascular function and blood pressure. Nat Med 2015;21:1028-1037

15. Acevedo L, Yu J, Erdjument-Bromage H, Miao RQ, Kim JE, Fulton D, Tempst P, Strittmatter SM, Sessa WC: A new role for Nogo as a regulator of vascular remodeling. Nat Med 2004;10:382-388

16. Kritz AB, Yu J, Wright PL, Wan S, George SJ, Halliday C, Kang N, Sessa WC, Baker AH: In vivo modulation of Nogo-B attenuates neointima formation. Mol Ther 2008;16:1798-1804

17. Ahn DG, Sharif T, Chisholm K, Pinto DM, Gujar SA, Lee PW: Ras transformation results in cleavage of reticulon protein Nogo-B that is associated with impairment of IFN response. Cell Cycle 2015;14:2301-2310

18. Rodriguez-Feo JA, Hellings WE, Verhoeven BA, Moll FL, de Kleijn DP, Prendergast J, Gao Y, van der Graaf Y, Tellides G, Sessa WC, Pasterkamp G: Low levels of Nogo-B in human

carotid atherosclerotic plaques are associated with an atheromatous phenotype, restenosis, and stenosis severity. Arterioscler Thromb Vasc Biol 2007;27:1354-1360

19. Miao RQ, Gao Y, Harrison KD, Prendergast J, Acevedo LM, Yu J, Hu F, Strittmatter SM, Sessa WC: Identification of a receptor necessary for Nogo-B stimulated chemotaxis and morphogenesis of endothelial cells. Proc Natl Acad Sci U S A 2006;103:10997-11002

20. Zhao B, Chun C, Liu Z, Horswill MA, Pramanik K, Wilkinson GA, Ramchandran R, Miao RQ: Nogo-B receptor is essential for angiogenesis in zebrafish via Akt pathway. Blood 2010;116:5423-5433

21. Zheng H, Xue S, Lian F, Wang YY: A novel promising therapy for vein graft restenosis: overexpressed Nogo-B induces vascular smooth muscle cell apoptosis by activation of the JNK/p38 MAPK signaling pathway. Med Hypotheses 2011;77:278-281

22. Schanda K, Hermann M, Stefanova N, Gredler V, Bandtlow C, Reindl M: Nogo-B is associated with cytoskeletal structures in human monocyte-derived macrophages. BMC Res Notes 2011;4:6

23. Park EJ, Grabinska KA, Guan Z, Sessa WC: NgBR is essential for endothelial cell glycosylation and vascular development. EMBO Rep 2016;17:167-177

24. Grimm D, Lee JS, Wang L, Desai T, Akache B, Storm TA, Kay MA: In vitro and in vivo gene therapy vector evolution via multispecies interbreeding and retargeting of adeno-associated viruses. Journal of virology 2008;82:5887-5911

25. Boels MG, Avramut MC, Koudijs A, Dane MJ, Lee DH, van der Vlag J, Koster AJ, van Zonneveld AJ, van Faassen E, Grone HJ, van den Berg BM, Rabelink TJ: Atrasentan Reduces Albuminuria by Restoring the Glomerular Endothelial Glycocalyx Barrier in Diabetic Nephropathy. Diabetes 2016;65:2429-2439

26. Satchell SC, Tasman CH, Singh A, Ni L, Geelen J, von Ruhland CJ, O'Hare MJ, Saleem MA, van den Heuvel LP, Mathieson PW: Conditionally immortalized human glomerular endothelial cells expressing fenestrations in response to VEGF. Kidney Int 2006;69:1633-1640

27. Saleem MA, O'Hare MJ, Reiser J, Coward RJ, Inward CD, Farren T, Xing CY, Ni L, Mathieson PW, Mundel P: A conditionally immortalized human podocyte cell line demonstrating nephrin and podocin expression. J AmSocNephrol 2002;13:630-638

28. Ko JM, Lung, M. L.: In vitro Human Umbilical Vein Endothelial Cells (HUVEC) Tube-formation Assay. In *Bio-protocol*, 2012, p. e260

29. Khoo CP, Micklem K, Watt SM: A comparison of methods for quantifying angiogenesis in the Matrigel assay in vitro. Tissue Eng Part C Methods 2011;17:895-906

30. Salmon AH, Ferguson JK, Burford JL, Gevorgyan H, Nakano D, Harper SJ, Bates DO, Peti-Peterdi J: Loss of the endothelial glycocalyx links albuminuria and vascular dysfunction. J Am Soc Nephrol 2012;23:1339-1350

31. Kobayashi T, Taguchi K, Yasuhiro T, Matsumoto T, Kamata K: Impairment of PI3-K/Akt pathway underlies attenuated endothelial function in aorta of type 2 diabetic mouse model. Hypertension 2004;44:956-962

32. Manning BD, Toker A: AKT/PKB Signaling: Navigating the Network. Cell 2017;169:381-405

33. Mariappan MM, Prasad S, D'Silva K, Cedillo E, Sataranatarajan K, Barnes JL, Choudhury GG, Kasinath BS: Activation of glycogen synthase kinase 3beta ameliorates diabetes-induced kidney injury. J Biol Chem 2014;289:35363-35375

34. Xiao L, Wang M, Yang S, Liu F, Sun L: A glimpse of the pathogenetic mechanisms of Wnt/beta-catenin signaling in diabetic nephropathy. Biomed Res Int 2013;2013:987064

35. MacDonald BT, Tamai K, He X: Wnt/beta-catenin signaling: components, mechanisms, and diseases. Dev Cell 2009;17:9-26

36. Marin EP, Moeckel G, Al-Lamki R, Bradley J, Yan Q, Wang T, Wright PL, Yu J, Sessa WC: Identification and regulation of reticulon 4B (Nogo-B) in renal tubular epithelial cells. Am J Pathol 2010;177:2765-2773

37. Tryggvason K, Patrakka J: Thin basement membrane nephropathy. J Am Soc Nephrol 2006;17:813-822

38. Staton CA, Reed MW, Brown NJ: A critical analysis of current in vitro and in vivo angiogenesis assays. Int J Exp Pathol 2009;90:195-221

39. Gurley SB, Clare SE, Snow KP, Hu A, Meyer TW, Coffman TM: Impact of genetic background on nephropathy in diabetic mice. Am J Physiol Renal Physiol 2006;290:F214-222

40. Hohenstein B, Hausknecht B, Boehmer K, Riess R, Brekken RA, Hugo CP: Local VEGF activity but not VEGF expression is tightly regulated during diabetic nephropathy in man. Kidney Int 2006;69:1654-1661

41. Oltean S, Qiu Y, Ferguson JK, Stevens M, Neal C, Russell A, Kaura A, Arkill KP, Harris K, Symonds C, Lacey K, Wijeyaratne L, Gammons M, Wylie E, Hulse RP, Alsop C, Cope G, Damodaran G, Betteridge KB, Ramnath R, Satchell SC, Foster RR, Ballmer-Hofer K, Donaldson LF, Barratt J, Baelde HJ, Harper SJ, Bates DO, Salmon AH: Vascular Endothelial Growth Factor-A165b Is Protective and Restores Endothelial Glycocalyx in Diabetic Nephropathy. J Am Soc Nephrol 2014;

42. Breier G, Albrecht U, Sterrer S, Risau W: Expression of vascular endothelial growth factor during embryonic angiogenesis and endothelial cell differentiation. Development 1992;114:521-532

43. Jo HN, Kang H, Lee A, Choi J, Chang W, Lee MS, Kim J: Endothelial miR-26a regulates VEGF-Nogo-B receptor-mediated angiogenesis. BMB Rep 2017;50:384-389

44. Kim HS, Skurk C, Thomas SR, Bialik A, Suhara T, Kureishi Y, Birnbaum M, Keaney JF, Jr., Walsh K: Regulation of angiogenesis by glycogen synthase kinase-3beta. J Biol Chem 2002;277:41888-41896

45. Skurk C, Maatz H, Rocnik E, Bialik A, Force T, Walsh K: Glycogen-Synthase Kinase3beta/beta-catenin axis promotes angiogenesis through activation of vascular endothelial growth factor signaling in endothelial cells. Circ Res 2005;96:308-318

46. Olsen JJ, Pohl SO, Deshmukh A, Visweswaran M, Ward NC, Arfuso F, Agostino M, Dharmarajan A: The Role of Wnt Signalling in Angiogenesis. Clin Biochem Rev 2017;38:131-142

47. Veelken R, Hilgers KF, Hartner A, Haas A, Bohmer KP, Sterzel RB: Nitric oxide synthase isoforms and glomerular hyperfiltration in early diabetic nephropathy. J Am Soc Nephrol 2000;11:71-79

48. Levine DZ: Hyperfiltration, nitric oxide, and diabetic nephropathy. Curr Hypertens Rep 2006;8:153-157

49. Kashihara N, Haruna Y, Kondeti VK, Kanwar YS: Oxidative stress in diabetic nephropathy. Curr Med Chem 2010;17:4256-4269

50. Daehn IS: Glomerular Endothelial Cells Stress and Cross-Talk With Podocytes in the Development of Diabetic Kidney Disease. Front Med (Lausanne) 2018;5:76

51. Takahashi T, Harris RC: Role of endothelial nitric oxide synthase in diabetic nephropathy: lessons from diabetic eNOS knockout mice. J Diabetes Res 2014;2014:590541

52. Veron D, Reidy KJ, Bertuccio C, Teichman J, Villegas G, Jimenez J, Shen W, Kopp JB, Thomas DB, Tufro A: Overexpression of VEGF-A in podocytes of adult mice causes glomerular disease. Kidney Int 2010;77:989-999

53. George B, Vollenbroker B, Saleem MA, Huber TB, Pavenstadt H, Weide T: GSK3beta inactivation in podocytes results in decreased phosphorylation of p70S6K accompanied by

cytoskeletal rearrangements and inhibited motility. Am J Physiol Renal Physiol 2011;300:F1152-1162

54. Dai C, Stolz DB, Kiss LP, Monga SP, Holzman LB, Liu Y: Wnt/beta-catenin signaling promotes podocyte dysfunction and albuminuria. J Am Soc Nephrol 2009;20:1997-2008

55. Zhang Y, Wang L, Zhang Y, Wang M, Sun Q, Xia F, Wang R, Liu L: Nogo-B Promotes Angiogenesis in Proliferative Diabetic Retinopathy via VEGF/PI3K/Akt Pathway in an Autocrine Manner. Cell Physiol Biochem 2017;43:1742-1754

56. Merscher-Gomez S, Guzman J, Pedigo CE, Lehto M, Aguillon-Prada R, Mendez A, Lassenius MI, Forsblom C, Yoo T, Villarreal R, Maiguel D, Johnson K, Goldberg R, Nair V, Randolph A, Kretzler M, Nelson RG, Burke GW, 3rd, Groop PH, Fornoni A, FinnDiane Study G: Cyclodextrin protects podocytes in diabetic kidney disease. Diabetes 2013;62:3817-3827

Table legend:

	non diabetic GFP	non diabetic sNogo-B	diabetic GFP	diabetic sNogo-B
HbA1c %(mmol/mol) (n=16-17/group)	4.5 (26) ± 1.7 (18)	4.3 (24) ± 1.5 (15)	7.7 (60) ± 2.2 (24)*	7.5 (59) ± 2.8 (30)**
BW (g) (n=18-20/group)	28.6 ± 2.9	27.5 ± 3.56	23.6 ± 3.9*	21.6±4.4**
SBP (mmHg) (n=7-10/group)	112 ± 11	111 ± 11	98 ± 9*	93±12**
Kidney weight/ BW (mg/g) (n=12-18/group)	8.7 ± 0.6	8.5 ± 0.6	9.9 ± 1.4*	10±1.2**
Glomerular volume (μm^3) (n=7-12/group, average 30 glomerular determinations per animal)	215480 ± 45972	231523 ± 38702	193193 ± 22518	239640 ± 51064

Table 1: DBA2J mice clinical and biochemical characteristic.

Clinical and biochemical characteristics in non-diabetic and diabetic DBA2/J mice overexpressing sNogo-B (sNogo-B) in the circulation or control vector (GFP). **BW**: body weight, **SBP**: systolic blood pressure. Data are expressed as mean±SD (ANOVA with post-hoc LSD: ND-GFP *vs* D-GFP, *p≤0.01; ND-sNogo-B vs D-sNogo-B, **p≤0.003).

Figures' legends:

Fig. 1: sNogo-B overexpression in the circulation ameliorates diabetic glomerulopathy. AAV-sNogo-B administration significantly increases plasma sNogo-B levels (**a**, n=12-21/group)(measured at sacrifice, 12-14 weeks post diabetes induction)(ND-GFP *vs* ND-sNogo-B, D-GFP *vs* D-sNogo-B, ~p≤0.0001) and ameliorates diabetes-mediated albuminuria (**b**, n=12-17/group), and hyperfiltration, measured as change in creatinine clearance (**c**, n=6-8/group). Diabetes was paralleled by an increase in sNogo-B in the urine (**d,** n=6/group), no differences were observed between mice with GFP or sNogo-B overexpression within the ND or D group (ND-GFP *vs* D-GFP, *p≤0.02; ND-sNogo-B *vs* D-sNogo-B, **p≤0.002; D-GFP *vs* D-sNogo-B, #p≤0.04). (**a, b, d**) Kruskal-Wallis and Mann-Whitney test (median interquartile range); (**c**) ANOVA with LSD post-hoc test (mean±SD). AAV-GFP treated mice black circles (●), AAV-sNogo-B treated mice white circles (○).

Fig. 2: sNogo-B overexpression in the circulation ameliorates diabetes-mediated glomerular ECs proliferation, reduction in glycocalyx lectin content and podocyte loss. (**a**) GECs proliferation was detected by $CD31^+/Ki67^+$ cells (white arrow). Diabetes significantly increases the average number of glomerular $CD31^+/Ki67^+$ cells by 7-fold which was reduced by sNogo-B overexpression in the circulation (**b**, n=8-12/group, average of 30-40 glomeruli/animal). Diabetes led to a 20% reduction in the thickness of the glycocalyx (assessed as lectin content) which was prevented by sNogo-B overexpression in the circulation (**c**, n=5/group, with 10-15 capillary loops studied per mouse). Similarly, diabetes-mediated glomerular podocytes loss was ameliorated by sNogo-B overexpression in the circulation (**d,** n=7-11/group). Elevated sNogo-B circulating levels had no effect on the diabetes-mediated increase in mesangial volume fraction (Vvmes)(**e**, n=9-12/group) or glomerular basement membrane (GBM) thickness (**f**, n=7-11/group).
(ND-GFP *vs* D-GFP, *p≤0.02; D-GFP *vs* D-sNogo-B, #p≤0.01; ND-sNogo-B *vs* D-sNogo-B, **p=0.02). ANOVA with LSD post-hoc test (mean±SD) for all comparisons. AAV-GFP treated mice black circles (●), AAV-sNogo-B treated mice white circles (○).

Fig. 3: sNogo-B overexpression in the circulation ameliorates diabetes-mediated VEGF-A/VEGFR2 signaling and eNOS^{Ser1177} phosphorylation in kidney cortex lysate.
Diabetes-induced kidney cortex VEGF-A expression (**a**, n=11-14/group, in duplicate) and phosphorylated p-VEGFR2^{Tyr1173} (**b**, n=7/group, in duplicate) was blunted in diabetic mice with sNogo-B overexpression in the circulation (ND-GFP *vs* D-GFP, *p≤0.003; D-GFP vs D-sNogo-B, #p≤0.03). Angpt-1/Angpt-2 ratio (**c**, n=7-8/group, in duplicate) was reduced in diabetes (ND-GFP *vs* D-GFP; ND-sNogo-B *vs* D-sNogo-B, *,**p≤0.03) but not altered by elevated sNogo-B circulating levels. The diabetes-mediated increase in ratio of phosphorylated p-

eNOS^{Ser1177}/total eNOS was prevented by sNogo-B overexpression in the circulation (**d**, n=8-10/group, ND-GFP *vs* D-GFP, *p=0.017; D-GFP *vs* D-sNogo-B, #p=0.05). (**e**) Representative data showing western blotting for phosphorylated p-eNOS^{Ser1177}, total eNOS and α-tubulin as housekeeping gene. ANOVA with LSD post-hoc test (mean±SD) for all comparisons. AAV-GFP treated mice black circles (●), AAV-sNogo-B treated mice white circles (○).

Fig. 4: sNogo-B overexpression in the circulation modulates diabetes-mediated AKT^{Ser473} and GSK3β^{Ser9} phosphorylation, while preventing diabetes-mediated β-catenin upregulation.

Diabetes was paralleled by a 2/3-fold increase in the ratio of phosphorylated p-AKT^{Ser473}/total AKT (**a,** n=6-8/group), a significant elevation of the ratio of phosphorylated p-GSK3β^{Ser9}/total GSK3β (**b,** n=8/group) and increased total β-catenin levels (**c,** n=8/group) in kidney cortex lysates (ND-GFP *vs* D-GFP, *p≤0.007). Diabetes-mediated AKT and GSK3β phosphorylation and upregulation β-catenin levels were partially or totally prevented by sNogo-B overexpression in the circulation (D-GFP *vs* D-sNogo-B, #p≤0.04; ND-sNogo-B *vs* D-sNogo-B, **p=0.0001). ANOVA with LSD post-hoc test (mean±SD) for all comparisons. AAV-GFP treated mice black circles (●), AAV-sNogo-B treated mice white circles (○).

Fig. 5. Full-length Nogo-B is expressed in glomeruli and sNogo-B overexpression in the circulation prevents diabetes-mediated Nogo-B downregulation.

(**a**) Electron microscopy showing the ultrastructure of the kidney glomerulus containing podocytes (POD), endothelial cells (EC) and the glomerular basement membrane (GBM). Immunogold labelling showed positive full-length Nogo-B expression in podocytes (black arrowheads) (**i**) and endothelial cells (black arrows) (**ii**). Collecting duct (medullary section) (**iii**) are used as positive control and negative control (omission of first antibody) is shown in (**iv**). Bar is 500 nm. (**b**) Positive signal for Nogo-B (right panel) is observed by immunohistochemistry both in glomerular cells (black arrows) and in the cortical collecting duct (positive internal control - red arrows) (magnification x40). Negative control-omission first anti-Nogo-B antiserum (left panel). (**c**) Full-length Nogo-B protein expression was downregulated in kidney cortex cell lysate and isolated glomeruli of diabetic mice and was prevented by AAV-sNogo-B overexpression in the circulation (**c**, n=10-13/group fort cortex lysate, n=4-5 for isolated glomeruli, ND-GFP *vs* D-GFP, *p≤0.045; D-GFP *vs* D-sNogo-B, #p≤0.015). (**d**) NgBR was detected in isolated glomeruli, no effect of diabetes or sNogo-B overexpression was noted. (**e**) Nogo-B expression (brown staining) was detected by immunohistochemistry in kidney biopsies from patients with diabetic nephropathy (DN) and thin basement membrane nephropathy (TBMN). Positive staining in the cortical collecting ducts serves as positive internal control (red arrows). Bar is 100 μm. Quantitative data showing the area of the glomerular tuft containing positive Nogo-B staining (n=10/group for

both TBMN and DN with an average score from 10 glomeruli obtained for each biopsy, TBMN *vs* DN, *p=0.0001). (**c, d**) ANOVA with LSD post-hoc test (mean±SD). AAV-GFP treated mice black circles (●), AAV-sNogo-B treated mice white circles (○); (**e**) Unpaired t-test (mean±SD).

Fig. 6: Incubation of GECs with high glucose and/or VEGF-A *in vitro* results in downregulation of full-length Nogo-B and parallel increase in sNogo-B secretion in the supernatant.

Fully differentiated GECs were incubated with normal (NG) or high (HG) glucose for 72h in the absence (vehicle: VEH) or presence of VEGF-A (50 ng/ml). Full-length Nogo-B protein expression was significantly downregulated by HG and/or VEGF-A (**a**, n=5-6, in duplicate). Conversely HG and/or VEGF-A was paralleled with an increase in sNogo-B levels, expressed as pg/ml·µg of cell protein, in the supernatant (**b**, n=4-5 in duplicate)(NG *vs* HG, NG *vs* VEGF-A, NG *vs* HG+VEGF-A, *p≤0.03). (**a**) ANOVA with LSD post-hoc test (mean±SD); (**b**) Kruskal-Wallis and Mann-Whitney test (median and interquartile range). NG+VEH black circles (●), HG+VEH white circles (○), NG+VEGF-A black square (■), HG+VEGF-A white square (□).

Fig. 7: sNogo-B overexpression in the supernatant ameliorates impaired angiogenesis in HUVEC cultured with serum from patients with type-1 diabetes mellitus and DN.

(**a**) HUVEC transfected with either ADV-control (cont) or ADV-sNogo-B (sNogo-B) were seeded onto Matrigel for tube formation assay. HUVEC were then incubated with media containing (4% vol/vol) sera obtained from blood of patients with type-1 diabetes mellitus susceptible (DN+) or protected (DN-) towards the progression of DN (**a**, n=16-18/group, in duplicate). An impairment in tube length (**b**) and number (**c**) was observed in HUVEC cultured with DN+ serum (ADV-control, DN+ *vs* DN-, *p≤0.04) was prevented by sNogo-B overexpression (DN+, ADV-control *vs* ADV-sNogo-B, #p≤0.02). (**d**) sNogo-B levels in the supernatant of HUVECs transfected with ADV-control (cont) or ADV-sNogo-B (sNogo-B) vectors (ADV-control *vs* ADV-sNogo-B within DN- and DN+, ~p≤0.0001, n=16-17/group, in duplicate). (**b, c**) ANOVA with LSD post-hoc test (mean±SD); (**d**) Kruskal-Wallis and Mann-Whitney test (median and interquartile range). ADV-control treated cells black circles (●), ADV-sNogo-B treated cells white circles (○).

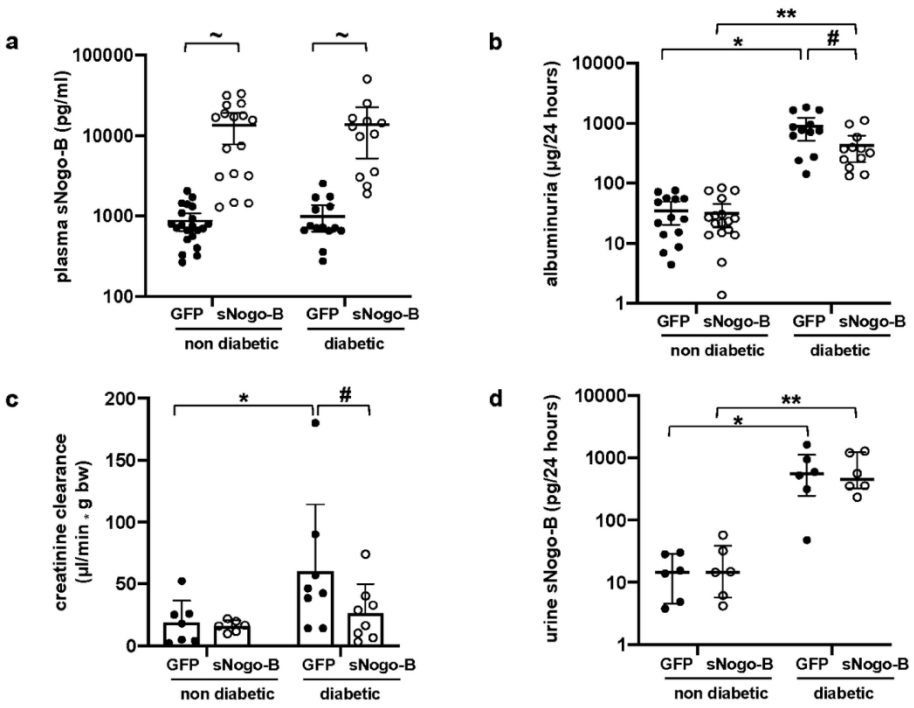

Fig. 1

135x95mm (300 x 300 DPI)

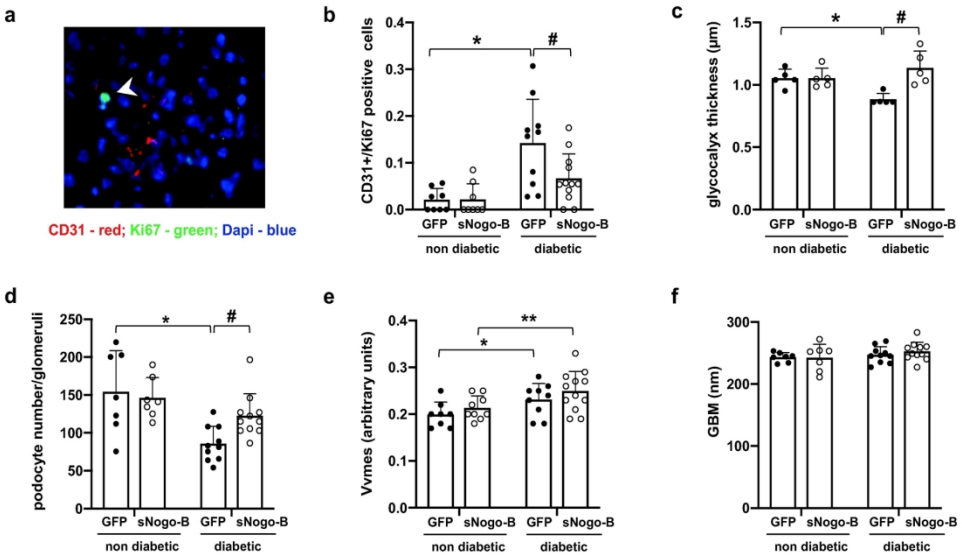

Fig. 2

172x100mm (300 x 300 DPI)

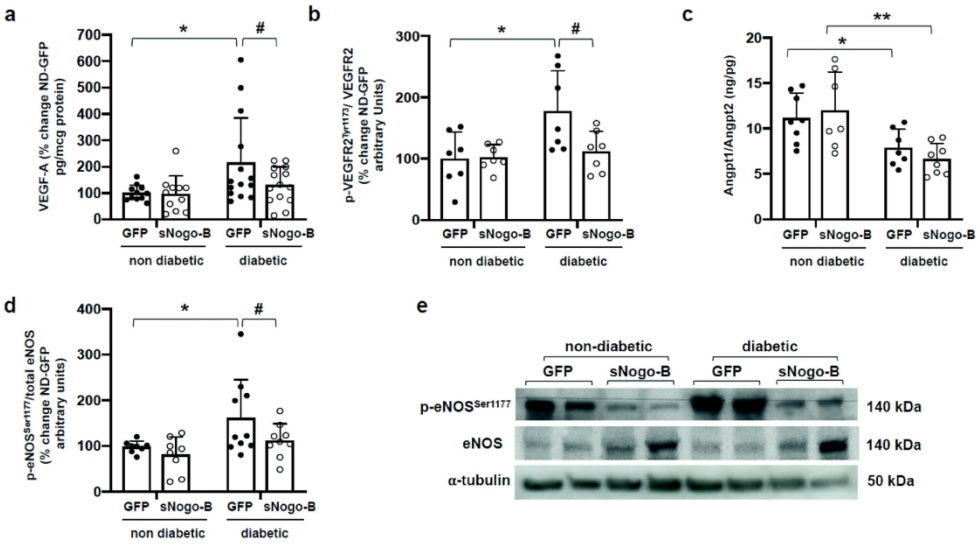

Fig. 3

173x94mm (300 x 300 DPI)

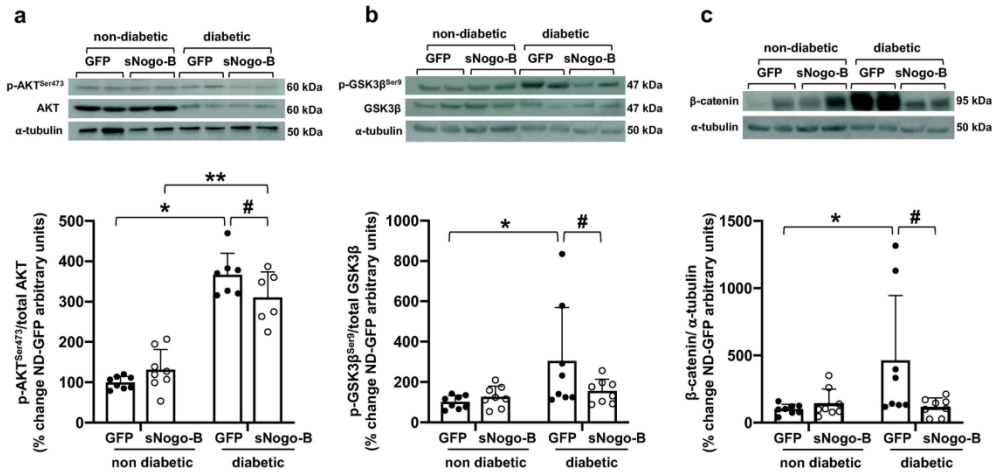

Fig. 4

159x90mm (300 x 300 DPI)

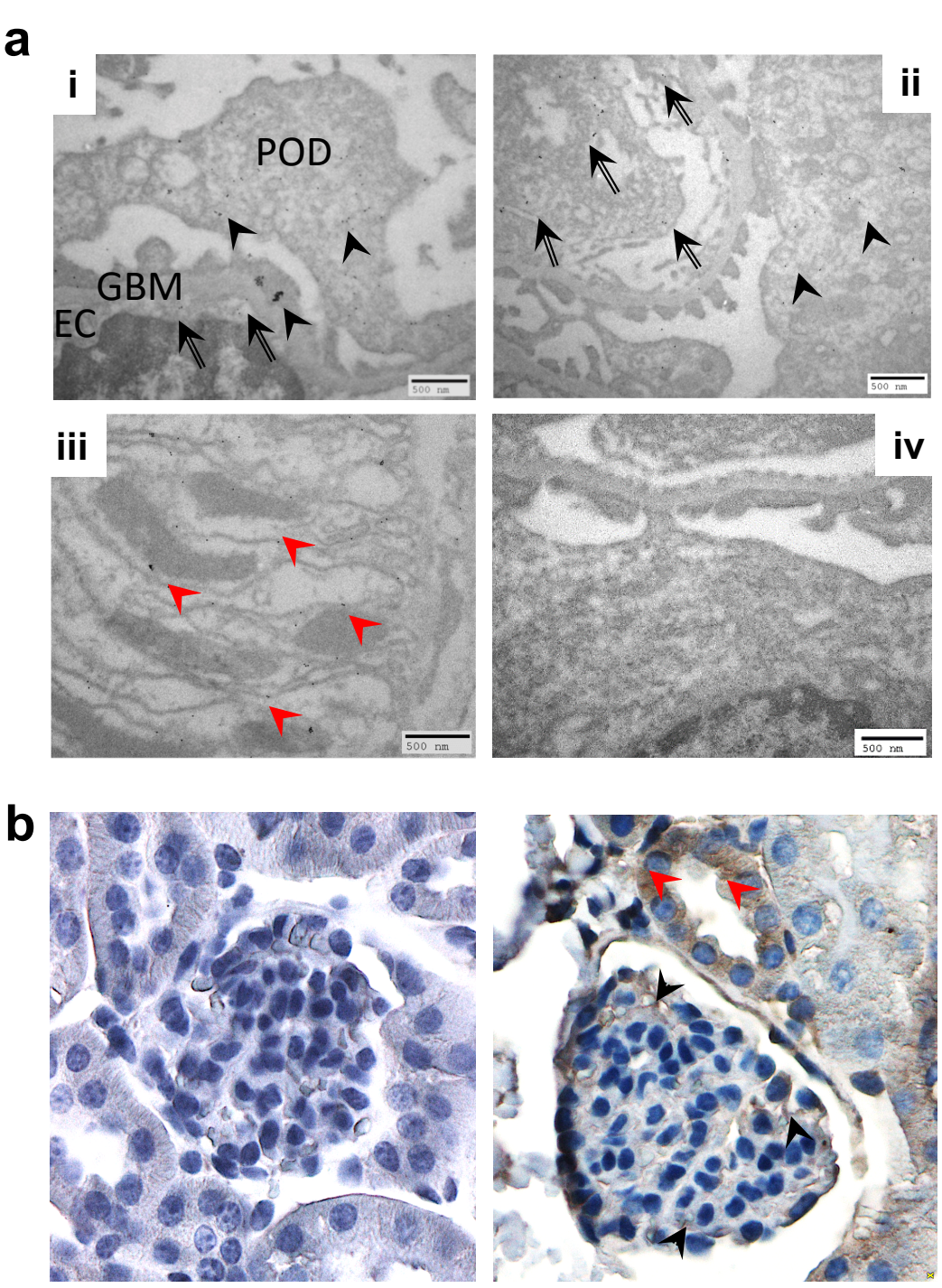

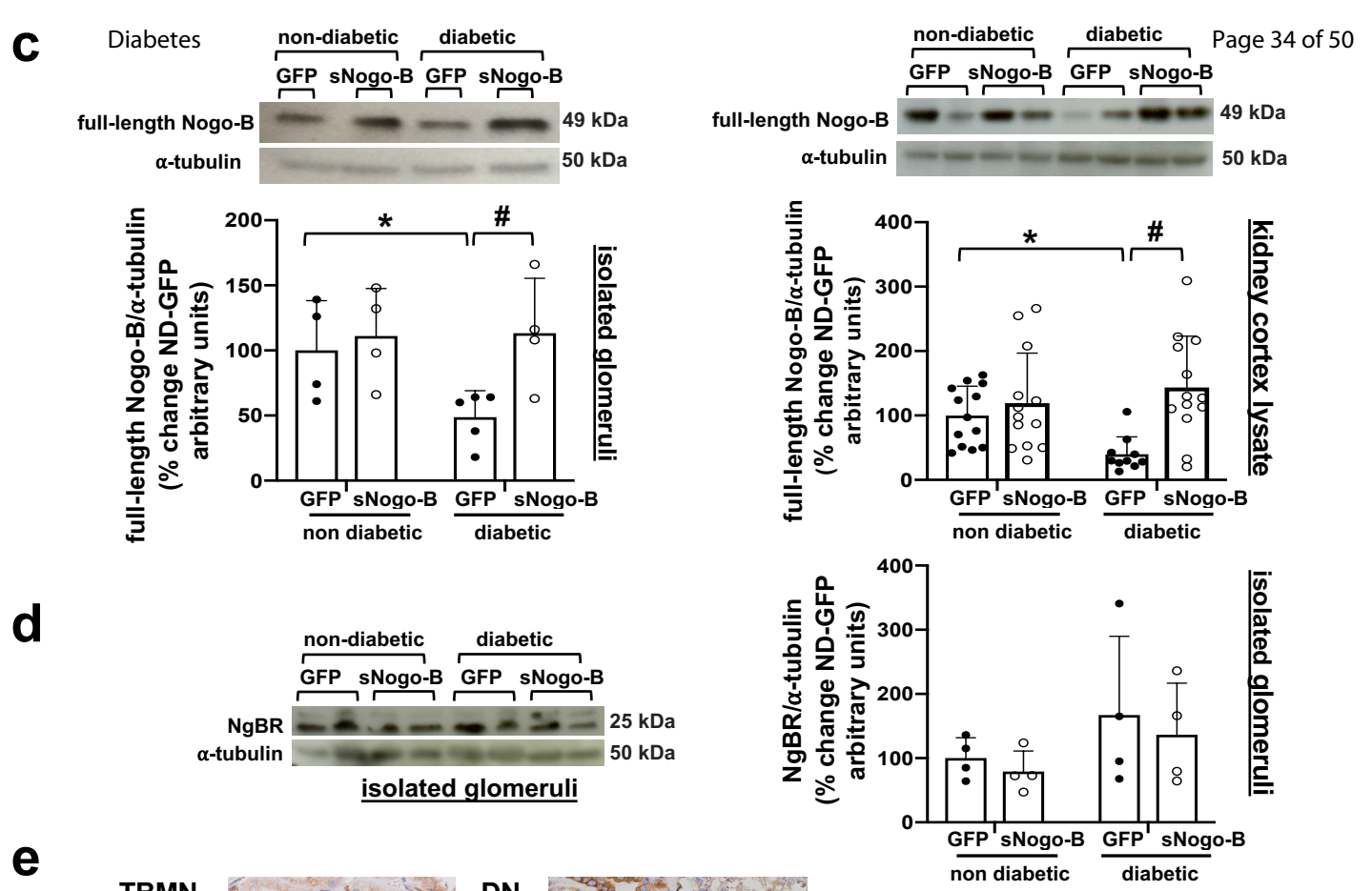

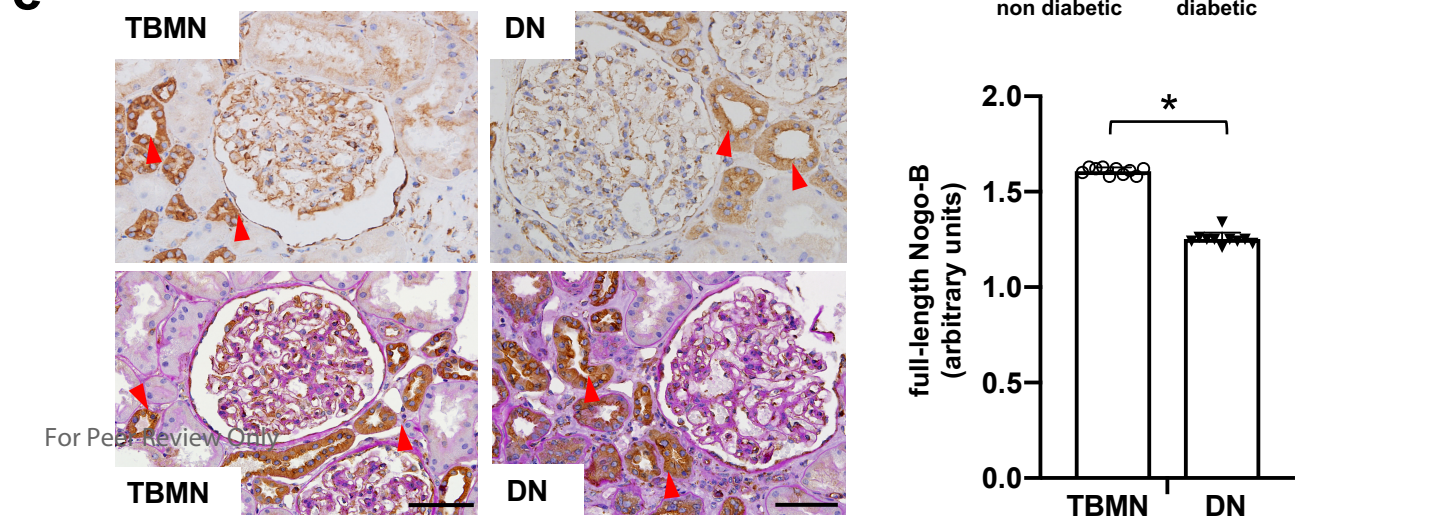

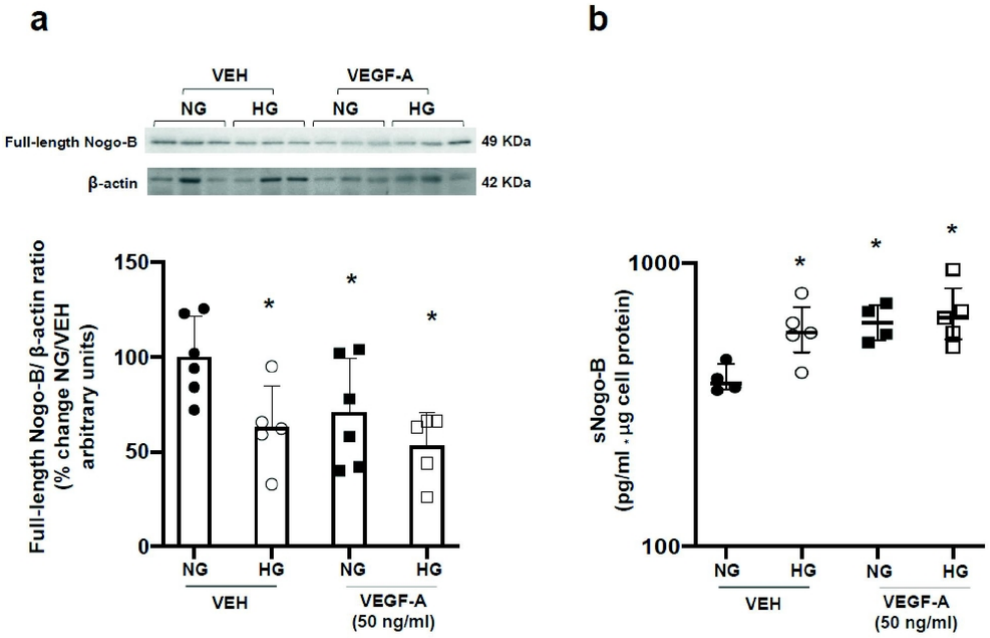

Fig. 6

84x56mm (300 x 300 DPI)

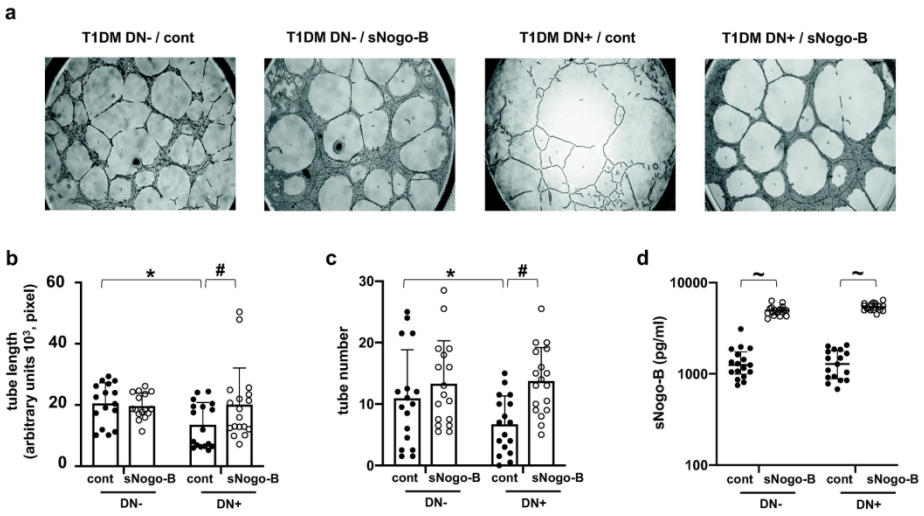

Fig. 7

174x98mm (300 x 300 DPI)

Supplemental Material

Generation of adeno-associated viral (AAV) vectors

The AAV-sNogo-B vector was generated by cloning the previously described (1) *HindIII/XhoI* 200aa N-terminus Nogo-B (sNogo-B) sequence cDNA in frame with the signal secretory sequence of placental alkaline phosphatase (AP), His tag, and placental AP coding region (gift of W Sessa, Yale University, CT, USA) downstream of the CMV promoter in AAV/DJ containing a hybrid capsid derived from eight wild-type AAV serotypes (2).

As control vector, we utilised an identical vector (AAV/DJ) driving (CMV promoter) the expression of green fluorescent protein (GFP). Viral particles were amplified commercially (Vectors Bioloab, Great Valley Parkway, Malvern, PA, USA).

AAV-sNogo-B and AAV-GFP vectors were administered intravenously at a dose of $1x10^{11}$ GC (gene copies) per mouse of 20gr (2).

Generation of adenoviral (ADV) vectors

Adenovirus (ADV)-sNogo-B vector (generated with the AdEasy Adenoviral Vector Systems, Agilent, Oxford, UK) expressed the described 200aa N-terminus Nogo-B (sNogo-B) sequence cDNA in frame with the signal secretory sequence of placental alkaline phosphatase (AP), His tag, and placental AP coding region (1)(gift of W Sessa, Yale University, CT, USA) under regulation of the CMV promoter, and was propagated in HEK293 cells and purified as previously described (3). As control ADV vector, we utilised an identical construct lacking sNogo-B cDNA. In experiments confluent cells were transfected with 100 multiplicity of infection (MOI).

Immunofluorescence

GECs proliferation (4). Frozen mouse kidneys, acetone fixed, 4μm sections were incubated with Alexa Fluor 594 conjugated anti-CD31 antibody (1:50)(Biolegend, London, UK) and Alexa Fluor 488 conjugated anti-Ki67 antibody (1:100)(Biolegend, London, UK) in PBS 1%BSA overnight in a humidified chamber at 4°C. Omission of the antisera and incubation with PBS 1%BSA served as a negative control. Sections were then washed in PBS and mounted with Vectashield antifade mounting medium with 4',6-diamidino-2-phenylindole (DAPI) (Vector Laboratories, Peterborough, UK). Glomerular Ki67/CD31 and CD31 positive ECs per glomerulus were visualised with Olympus BX51 fluorescent microscope.

Endothelial glycocalyx determination. Frozen kidney 4μm sections were obtained from each animal and left to air-dry overnight at RT. Kidney sections were then fixed in acetone at -20°C for 10min and left to air-dry for 20min. Sections were incubated overnight at 4°C with 0.2μg/ml

FITC-conjugated lectin from *Lycopersicon Esculentum Agglutinin* (LEA)(Sigma)(1:2500) in PBS 1%BSA for glycocalyx staining and 1µg/ml mouse monoclonal CD31 antibody (Santa Cruz Biotechnology, Heidelberg, Germany)(1:1000) in PBS 1%BSA for ECs staining.
Following this, sections were incubated for 1h with 1µg/ml (1:1000 dilution in PBS 1%BSA) Alexa Fluor 568-conjugated goat anti-mouse IgG (ThermoFisher Scientific, Oxford, UK). Slides were washed between steps with PBS and mounted with Vectashield antifade mounting medium with DAPI (Vector Laboratories, Peterborough, UK).
Capillaries were then analysed by confocal microscopy (Eclipse Ti-E Inverted, Nikon, https://www.kcl.ac.uk/innovation/research/corefacilities/smallrf/nikon/index.aspx) with NIS-Elements Viewer elements software. Multiple glomeruli in each kidney sample were captured at 40x magnification.
To establish the glycocalyx thickness, images were analysed with ImageJ software (NIH-Bethesda, MD, USA). Glomerular capillary loops were identified in each glomeruli and fluorescent intensity plots, for CD31 and intraluminal LEA, were processed from a line perpendicular to the capillary wall. The distance from the peak of CD31 signal to the half-maximal intensity of the intraluminal LEA peak, representing the endothelial glycocalyx thickness, was expressed in µm as previously described (5; 6).

Electron microscopy and glomerular ultrastructure analysis

Mesangial volume fraction, as an index of glomerular extracellular matrix deposition, GBM thickening, were studied with electron microscopy stoichiometry techniques as described (7; 8).
Specifically, mesangial volume fraction was estimated using point counting. A grid of coarse and fine points (ratio 1:8) was overlaid on each image. The number of coarse points hitting the reference space (the glomerular tuft as defined by the minimal string polygon) and fine points on mesangium were counted. The volume fraction of mesangium was calculated as follows: $Vv = Pmes/(Pglom * 8)$ where Pmes is the number of points on mesangium and Pglom is the number of points on the glomerular tuft.
Glomerular basement membrane width was measured directly on images using the line tool. In order to select, without bias, the portion of GBM that was measured, a grid of lines was superimposed on each image. The GBM was measured wherever a grid line intersected with the endothelium, perpendicular to the endothelium.
Podocyte number was estimated from electron micrographs by first estimating podocyte density (Nv) using the method of Weibel and Gomez (9) $NV = K/\beta \sqrt{N_A^3/V_v}$, where N_A is the profile density of the particles, V_v is the volume fraction of the particles, K is a size distribution coefficient and β is a shape constant. For most biological applications the size distribution

coefficient, K, varies between 1 and 1.05 and can therefore be neglected. The shape constant used for podocyte nuclei is for an ellipsoid, 1.55. Podocyte density was multiplied by glomerular volume to give podocyte number $N = N_V * V$.

This method has been shown to be comparable to the disector/fractionator method (8), which is considered to be the gold-standard.

Glomerular volume was calculated as described previously in rodents by glomerular diameter determination in paraformaldehyde fixed tissue (10).

sNogo, VEGF-A, Angpt1/2 and VEGFR2^{Tyr1173} phosphorylation ELISA

All ELISA experiments were conducted in duplicate on plasma, urine and cell culture media for sNogo-B. For cortex VEGF-A, Angpt1/2, and VEGFR2^{Tyr1173} phosphorylation, 50µg of total cortex cells lysate was assessed in duplicate for each animal. The ELISA kit utilised for VEGFR2 phosphorylation recognises the human VEGFR2^{Tyr1175} known to be identical to residue VEGFR2^{Tyr1173} in the mouse (11).

Immunoblotting

Cells or tissues (mouse renal cortex) were homogenised in RIPA lysis buffer (ThermoFisher scientific, Oxford, UK) containing proteases and phosphatases inhibitors, and lysates were separated by 10% SDS-PAGE. Immunoreactive bands were visualized with chemiluminescence and quantified using densitometry with α-tubulin or β-actin as house-keeping proteins control as previously described (12).

Culture and characterization of mouse lung endothelial cells

Primary lung ECs were isolated from adult C57BL/6J mice and cultured as previously described (13; 14) after two cells' sorting with CD31 antisera (monoclonal rat anti-Mouse CD31 antiserum, BD Pharmingen/Biosciences, Wokingham, UK) and sheep anti-rat IgG coated Dynabeads (M-450 Dynabeads, Dynal Biotech, ThermoFisher Scientific, Oxford, UK). Lung ECs were cultured up to three passages. Lung EC characterisation was conducted with immunofluorescence, in 4% paraformaldehyde fixed (10min) permeabilised (0.5% triton in PBS 10min) EC using anti eNOS rabbit polyclonal antiserum (Santa Cruz Biotechnology, Heidelberg, Germany) at 4°C for 12h followed by incubation with anti-rabbit Alexa 594 secondary antibody respectively (ThermoFisher Scientific, Oxford, UK). Slides were washed between steps with PBS and mounted with Vectashield antifade mounting medium with DAPI (Vector Laboratories, Peterborough, UK). These cells were utilised as positive control for the expression of NgBR (15).

Human GECs (gift from S Satchell, University of Bristol, UK) were cultured in EGM-2MV medium (Lonza, CC-3202) and differentiated as previously described (16).

Immunoprecipitation (IP) and proximity ligation assay (PLA) experiments

For IP experiments, whole protein cell lysates were obtained from human GECs overexpressing sNogo-B (6xHis-Tag/sNogo-B construct) and incubated with either rabbit polyclonal anti NgBR antisera (1µg)(Novus Biological, Oxford, UK), or anti 6xHis-Tag (1µg) mouse monoclonal antiserum (ThermoFisher Scientific, Oxford, UK), or vehicle IgG (1µg). Immunoprecipitates were then obtained by incubation with protein G-coated magnetic beads as per standard protocol (Universal Magnetic Co-IP Kit, Active Motive). Immunoblotting was then conducted with anti 6xHis-Tag and anti NgBR antisera.

For the PLA experiments (Duolink Sigma, Gillingham, UK) we followed the manufacturer instructions. NgBR-sNogo-B interaction was studied with PLA probes (one PLUS and one MINUS) with hosts corresponding to each of the primary antibodies (anti-rabbit and anti-mouse), and interaction visualised with immunofluorescence following manufacturer instructions (Duolink® In Situ Red Starter Kit Mouse/Rabbit). GECs were visualised with mouse monoclonal anti VE-cadherin antibody (Santa Cruz Biotechnology, Heidelberg, Germany) in PBS 1%BSA and secondary goat anti mouse Alexa 488 (ThermoFisher Scientific, Oxford, UK). Negative controls for the PLA consisted of omission of each of the two primary antibodies used (one negative control without anti N-terminus NgBR, and one without anti 6xHis-Tag, not shown).

Nogo-B immunogold staining in glomeruli

Nogo-B immunogold staining was conducted in mouse renal cortex tissue fixed in 2% paraformaldehyde. Briefly ultrathin sections (70nm) were incubated overnight at 4°C with sheep polyclonal anti-Nogo-B (N-terminus) antibody (R&D System, Abingdon, UK) diluted 1:200 in phosphate buffer saline (PBS), 0.5% bovine serum albumin (BSA), followed by gold-conjugated goat anti-sheep IgG (1:20) in PBS 0.5%BSA for 1h at RT. Grids that had not been incubated with primary antibody were used as negative controls. Samples were examined with a Philips CM100 Transmission electron microscopy.

Nogo-B immunohistochemistry

Human tissue: Human archival formalin-fixed/paraffin embedded kidney biopsies, obtained from the National Clinical Research Centre of Kidney Disease and Guangdong Provincial Institute of Nephrology, Guangzhou-China between 2013 to 2015, were used for Nogo-B immunohistochemistry staining. The study was specifically approved by the Ethics Committee

of National Clinical Research Centre of Kidney Disease and Guangdong Provincial Institute of Nephrology in Guangzhou, China.

The indications for performing the renal biopsy in patients with type 2 diabetes (T2DM) followed internal guidelines whereby renal biopsy was indicated in the presence of macroproteinuria with or without microscopic haematuria or rapid progressive decline in renal function. The indication for renal biopsy for patients with thin basement membrane nephropathy (TBMN) was microscopic haematuria. Histological diagnosis of diabetic nephropathy (DN) and TBMN had been undertaken by two independent renal pathologists, and no evidence of other renal diseases and no history of assumption of herbal medicines or other nephrotoxic agents was noted. Patients characteristic are described in **Table 1**.

Two-μm thick paraffin sections were studied using the standard streptavidin-biotin complex method using a specific sheep polyclonal anti Nogo-B N-terminus antibody (1:50)(R&D System, Abingdon, UK) at 4°C for 12h followed by incubation with biotin-conjugated goat anti-sheep secondary antibody (1:200, Dako; Ely, UK) for 30min at RT and peroxidase reaction with 3,3'-diaminobenzidine tetra-hydrochloride (Dako, Carpinteria, CA, USA). Nuclei were counterstained with haematoxylin and slides mounted in Permount mounting medium (eBioscience, San Diego, CA, USA). For visualization, another set of sections was counterstained with Periodic Acid-Schiff. Staining of cortical collecting duct served as internal positive controls for Nogo-B staining. Omission of primary antibody served as a negative control (not shown).

Nogo-B expression level was assessed semi quantitatively. Glomerular boundaries were defined by external perimeter of the capillary loops. The proportional area occupied by immunoreactive Nogo-B was calculated using a computer assisted KS-300 image analysis system (Carl-Zeiss, Jena, Germany) connected to an BX51 microscope (Olympus, Tokyo, Japan) and a KY-F55B colour video camera (JVC, Tokyo, Japan). Determinations were made at the same light microscope intensity.

Mouse tissue: similar immunohistochemistry techniques were utilised for mouse kidney tissue. Omission of first antiserum served as negative control and slide were stained with haematoxylin as per standard protocol.

Culture of Human umbilical vein endothelial cells (HUVEC) and tube formation assay

HUVECs were cultured with EGM-MV medium (PromoCell, Heidelberg, Germany) and cultured up to third passage. After transfection (ADV-sNogo-B and ADV-control vector) cells were trypsinised from tissue culture flasks and then plated in 96 well plates (5000 cells/well) in EGM basal media containing patients' sera (4% vol/vol)(see below) and tube formation performed on Matrigel (BD Biosciences, UK) previously described.

Patients sera was collected, after consent, from patients with type-1 diabetes (T1DM) with or without DN identified within the Department of Diabetes and Endocrinology at Guy's and St Thomas NHS foundation Trust, London, UK. T1DM was defined as onset before age 35, insulin therapy within 6 months of diagnosis and no breaks in insulin therapy for more than 6 months (17). DN was defined as albuminuria or history of clinical albuminuria (18) in at least two of three overnight urine collections, in the absence of other causes of renal damage or urinary tract infections, but in the presence of retinopathy. The patients with T1DM and minimal disease progression were defined as patients with ≥20 years of diabetes duration, normoalbuminuria, normal serum creatinine, and normal blood pressure (≤130/80mmHg). All diabetic patients had normal to mild impairment of renal function (eGFR, assessed with MDRD (19) formula, >60 ml/min/1.73m^2) with (DN+) or without (DN-) presence or history of microalbuminuria (20). Statin treatment was higher in the DN+ group; all recruited patients were non-smokers, and absence of history of acute ischemic events (e.g. myocardial infarction, stroke) was ensured in all patients (**Table 2**). The study was approved by the national Health Research Authority. Blood was collected in the non-fasting state and serum was stored at -80°C.

Figures

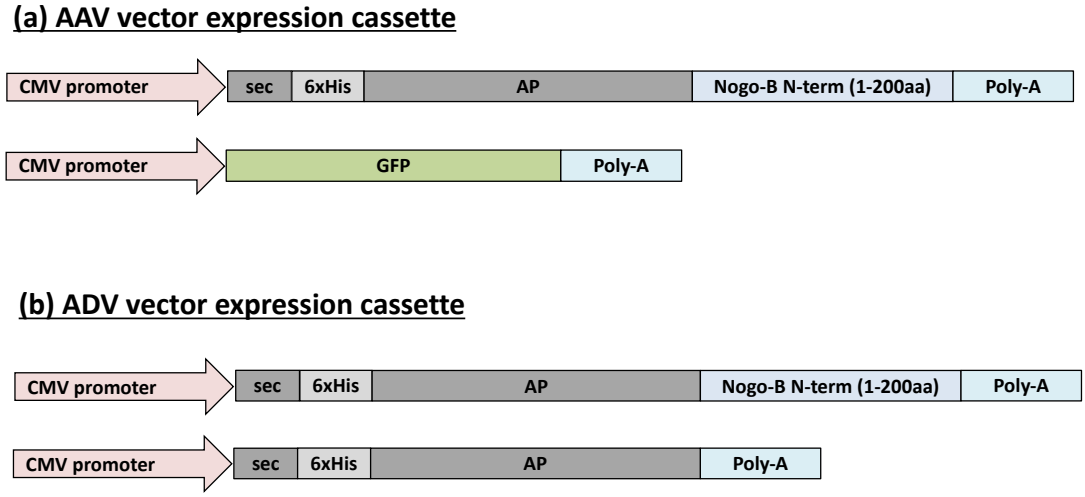

AAV: Adeno associated vector.
ADV: Adenoviral vector.
CMV promoter: citomegalovirus promoter.
sec: secretory signal alkaline phosphatase.
AP: alkaline phosphatase (~1.6 Kb, ~60-65 kDA), from pSEAP (*Clontech*).
6xHis: Histidine Tagx6 (~1 kDA).
Poly-A: polyadenylation signal.
Nogo-B N-term (1-200aa): predicted 15-20 kDA.

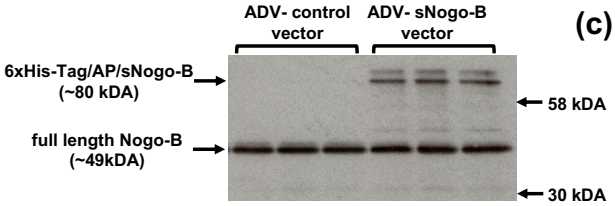

Total cells lysate of HUVEC transfected with either ADV-control or ADV-sNogo-B vector (immunoblotting with anti N-terminus Nogo-B antisera).

Fig. 1: Schematic representation of viral vectors transcription cassettes (not in scale). Schematic graphical representation of transcription cassette utilized in the AAV (**a**) and ADV (**b**) viral vectors. In (**c**) is presented the estimated molecular weight of the transgene (~80 kDA) in total cell lysate obtained from HUVEC transfected with ADV-control or ADV-sNogo-B vector.

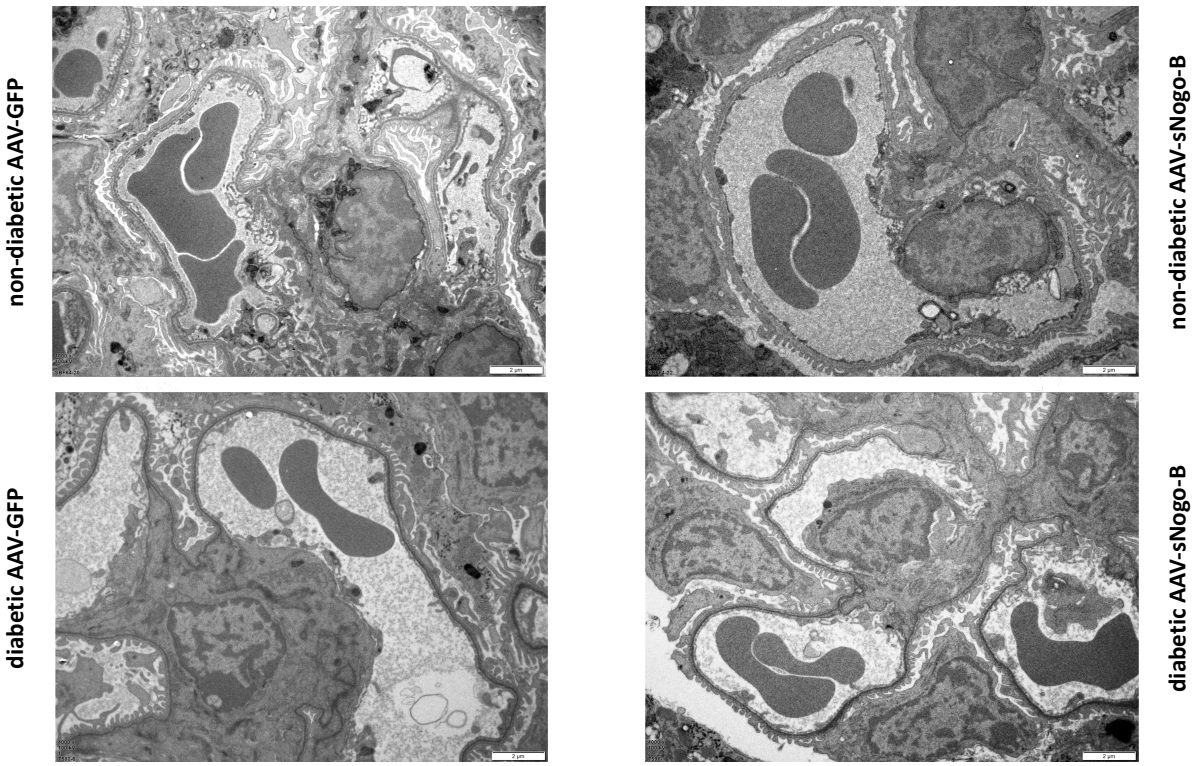

Fig. 2: Representative EM scanning images from control and diabetic mice with or without sNogo-B overexpression in the circulation.

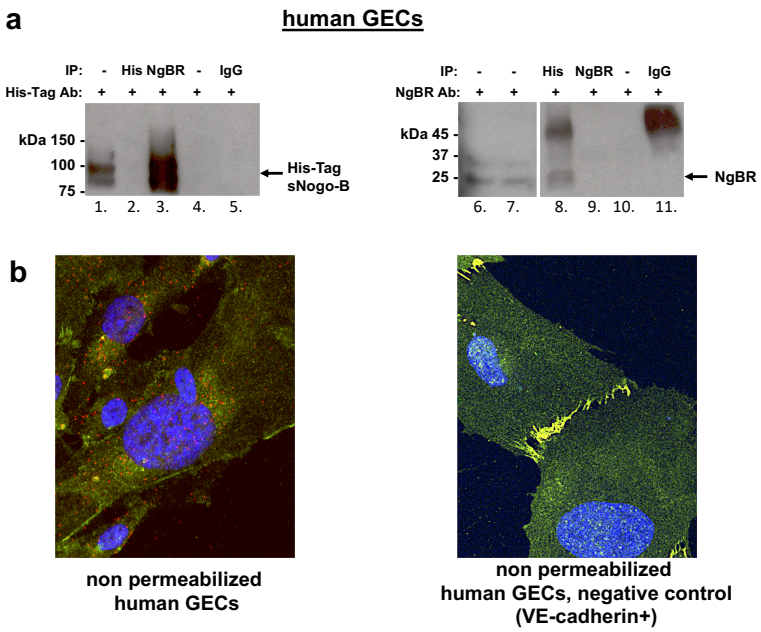

Fig. 3: sNogo-B interacts with NgBR in GECs *in vitro*.

(**a**) sNogo-B/NgBR interaction was demonstrated with immunoprecipitation in 6xHis-Tag/sNogo-B overexpressing human GECs. Western blot analysis for His-Tag (left blots) and NgBR (right blots) after NgBR and His-Tag immunoprecipitation from total GECs' lysate. (Lane 1. and 6. total GECs' lysate, 4. and 10. no IP, 5. and 11. control IgG, lane 7 mouse lung ECs (positive control for NgBR expression). (**b**) ECs' sNogo-B/NgBR interaction was visualised (red/orange dots) with proximity ligation assay in non-permeabilized human GECs after 1 min incubation with "conditioned media" containing 6xHis-Tag/sNogo-B protein (~6000 pg/ml); no signal was observed in negative controls where the VE-cadherin positive staining (green) was visible.

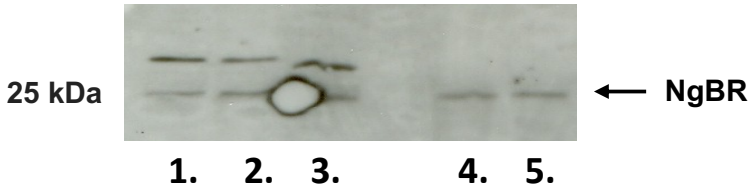

1. , 2. - diffentiated human podocytes
3. - proliferating human podocytes
4. , 5. - kidney cortex total cells lysate (positive control)

Fig. 4: Podocytes express NgBR *in vitro*

Tables:

	Controls (TBMN)	Patients with diabetes
Sex	1M 9F	8M 2F
Age (years)	33 ± 5	48 ± 10
Duration Diabetes (years)		5.8 ± 2.7
HbA_{1c} % (mmol/mol)		7.3 (56.0) ± 1.2 (13.6)
BP systolic (mmHg)	121 ± 10	144 ± 20
BP diastolic (mmHg)	74 ± 10	89.7 ± 10
eGFR (ml/min/1.73 m^2)	117 ± 8.7	107 ± 14
Proteinuria (g/24h)*	0.13 [0.08-0.21]	2.17 [0.88-4.76]
Retinopathy (%)		40

Table 1: Patients with DN or TBMN clinical characteristics.

Renal biopsies obtained from patients with T2DM and TBMN were studied. eGFR calculated with MDRD formula. Data are expressed as mean±SD, *median [interquartile range].

	T1DM / DN-	T1DM / DN+
Sex	8M 9F	11M 7F
Age (years)	46.8 ± 12.2	53.3 ± 10.8
Duration Diabetes (years)	31 ± 11.4	30.4 ± 10.2
HbA_{1c} % (mmol/mol)	7.9 (62.7) ± 1.2 (13.0)	7.8 (61.8) ± 1.1 (12.6)
BP systolic (mmHg)	130.2 ± 15.1	140.8 ± 13.1
BP diastolic (mmHg)	76.6 ± 8.7	75.9 ± 6.8
Cholesterol (mmol/L)	4.7 ± 0.8	4.05 ± 0.6
eGFR (ml/min/1.73 m^2)	101.7 ± 22.6	81.8 ± 32.2
ACR (g/mol)*	0.8 [0.4-2.1]	1.15 [0.6-9.3]
RAAS inhibition (%)	0	100
Statin (%)	29	70
Retinopathy (%)	100	100
Smoking (%)	0	0
sNogo-B (pg/ml)*	420.7 [270.6-883.2]	463.8 [293.5-658.9]

Table 2: Patients with type-1 diabetes, with (DN+) or without (DN-) history of albuminuria, clinical characteristics.

Patients with type-1 diabetes (T1DM) with (DN+) or without (DN-) history of albuminuria were enrolled in the study. eGFR calculated with MDRD formula. Data are expressed as mean ± SD, *median [interquartile range].

References:

1. Miao RQ, Gao Y, Harrison KD, Prendergast J, Acevedo LM, Yu J, Hu F, Strittmatter SM, Sessa WC: Identification of a receptor necessary for Nogo-B stimulated chemotaxis and morphogenesis of endothelial cells. Proc Natl Acad Sci U S A 2006;103:10997-11002

2. Grimm D, Lee JS, Wang L, Desai T, Akache B, Storm TA, Kay MA: In vitro and in vivo gene therapy vector evolution via multispecies interbreeding and retargeting of adeno-associated viruses. Journal of virology 2008;82:5887-5911

3. Mallawaarachchi CM, Weissberg PL, Siow RC: Smad7 gene transfer attenuates adventitial cell migration and vascular remodeling after balloon injury. Arterioscler Thromb Vasc Biol 2005;25:1383-1387

4. Dessapt-Baradez C, Woolf AS, White KE, Pan J, Huang JL, Hayward AA, Price KL, Kolatsi-Joannou M, Locatelli M, Diennet M, Webster Z, Smillie SJ, Nair V, Kretzler M, Cohen CD, Long DA, Gnudi L: Targeted Glomerular Angiopoietin-1 Therapy for Early Diabetic Kidney Disease. J Am Soc Nephrol 2014;25(1):33-42

5. Boels MG, Avramut MC, Koudijs A, Dane MJ, Lee DH, van der Vlag J, Koster AJ, van Zonneveld AJ, van Faassen E, Grone HJ, van den Berg BM, Rabelink TJ: Atrasentan Reduces Albuminuria by Restoring the Glomerular Endothelial Glycocalyx Barrier in Diabetic Nephropathy. Diabetes 2016;65:2429-2439

6. Dane MJ, van den Berg BM, Avramut MC, Faas FG, van der Vlag J, Rops AL, Ravelli RB, Koster BJ, van Zonneveld AJ, Vink H, Rabelink TJ: Glomerular endothelial surface layer acts as a barrier against albumin filtration. Am J Pathol 2013;182:1532-1540

7. White KE, Bilous RW: Type 2 diabetic patients with nephropathy show structural-functional relationships that are similar to type 1 disease. JAmSocNephrol 2000;11:1667-1673

8. White KE, Bilous RW: Estimation of podocyte number: a comparison of methods. Kidney Int 2004;66:663-667

9. Weibel ER, Gomez DM: A principle for counting tissue structures on random sections. JApplPhysiol 1962;17:343-348

10. Steffes MW, Brown DM, Basgen JM, Mauer SM: Amelioration of mesangial volume and surface alterations following islet transplantation in diabetic rats. Diabetes 1980;29:509-515

11. Sakurai Y, Ohgimoto K, Kataoka Y, Yoshida N, Shibuya M: Essential role of Flk-1 (VEGF receptor 2) tyrosine residue 1173 in vasculogenesis in mice. Proc Natl Acad Sci U S A 2005;102:1076-1081

12. Ku CH, White KE, Dei CA, Hayward A, Webster Z, Bilous R, Marshall S, Viberti G, Gnudi L: Inducible overexpression of sFlt-1 in podocytes ameliorates glomerulopathy in diabetic mice. Diabetes 2008;57:2824-2833

13. Cantalupo A, Zhang Y, Kothiya M, Galvani S, Obinata H, Bucci M, Giordano FJ, Jiang XC, Hla T, Di Lorenzo A: Nogo-B regulates endothelial sphingolipid homeostasis to control vascular function and blood pressure. Nat Med 2015;21:1028-1037

14. Allport JR, Lim YC, Shipley JM, Senior RM, Shapiro SD, Matsuyoshi N, Vestweber D, Luscinskas FW: Neutrophils from MMP-9- or neutrophil elastase-deficient mice show no defect in transendothelial migration under flow in vitro. J Leukoc Biol 2002;71:821-828

15. Park EJ, Grabinska KA, Guan Z, Sessa WC: NgBR is essential for endothelial cell glycosylation and vascular development. EMBO Rep 2016;17:167-177

16. Satchell SC, Tasman CH, Singh A, Ni L, Geelen J, von Ruhland CJ, O'Hare MJ, Saleem MA, van den Heuvel LP, Mathieson PW: Conditionally immortalized human glomerular endothelial cells expressing fenestrations in response to VEGF. Kidney Int 2006;69:1633-1640

17. American Diabetes A: 2. Classification and Diagnosis of Diabetes: Standards of Medical Care in Diabetes-2018. Diabetes Care 2018;41:S13-S27

18. Borch-Johnsen K, Nissen H, Salling N, Henriksen E, Kreiner S, Deckert, Nerup J: The natural history of insulin-dependent diabetes in Denmark: 2. Long-term survival--who and why. Diabetic Medicine 1987;4:211-216

19. Levey AS, Coresh J, Greene T, Stevens LA, Zhang YL, Hendriksen S, Kusek JW, Van LF: Using standardized serum creatinine values in the modification of diet in renal disease study equation for estimating glomerular filtration rate. AnnInternMed 2006;145:247-254

20. Dessapt C, Karalliedde J, Hernandez-Fuentes M, Martin PP, Maltese G, Dettani N, Atkar R, Viberti G, Gnudi L: Circulating Vascular Progenitor Cells in patients with Type 1 Diabetes and Microalbuminuria. Diabetes Care 2010;33:875-877